ABSTRACT

BURMESTER CURVE AND NUMERICAL MOTION GENERATION OF GRASHOF MECHANISMS WITH PERIMETER AND TRANSMISSION ANGLE OPTIMIZATION IN MATHCAD

by
Peter J. Martin

An infinite number of planar four-bar mechanism solutions exist for a series of prescribed rigid-body positions. Given a set of Burmester curves or numerically-generated fixed and moving pivot curves, sorting through the limitless number of possible mechanism solutions to find one that ensures full link rotatibility, satisfies compactness criteria and produces feasible transmission angles can be a daunting task. In this work, two algorithms are developed and presented by which the user can select optimum planar four-bar motion generators (optimum with respect to Grashof criteria, mechanism perimeter criteria and transmission angle criteria) from a set of all mechanism solutions produced by through either Burmester curves or numerically-generated fixed and moving curves. Both the Burmester curve-based method and the numerical fixed and moving pivot curve-based method have been codified in MathCAD to support advanced analysis capabilities. The examples in this work demonstrate the synthesis of optimum Grashof crank-rocker, drag link, double-rocker and triple-rocker motion generators.

BURMESTER CURVE AND NUMERICAL MOTION GENERATION OF GRASHOF MECHANISMS WITH PERIMETER AND TRANSMISSION ANGLE OPTIMIZATION IN MATHCAD

by
Peter J. Martin

A Thesis
Submitted to the Faculty of
New Jersey Institute of Technology
in Partial Fulfillment of the Requirements for the Degree of
Master of Science in Mechanical Engineering

Department of Mechanical Engineering

January 2007

APPROVAL PAGE

BURMESTER CURVE AND NUMERICAL MOTION GENERATION OF GRASHOF MECHANISMS WITH PERIMETER AND TRANSMISSION ANGLE OPTIMIZATION IN MATHCAD

Peter J. Martin

Dr. Rajpal S. Sodhi, Dissertation Advisor — Date
Professor of Mechanical Engineering, NJIT

Dr. Ian S. Fischer , Committee Member — Date
Professor of Mechanical Engineering, NJIT

Dr. Kevin Russell, Committee Member — Date
Adjunct Professor of Mechanical Engineering, NJIT

BIOGRAPHICAL SKETCH

Author: Peter J. Martin

Degree: Master of Science

Date: January 2007

Undergraduate and Graduate Education:

- Master of Science in Mechanical Engineering,
  New Jersey Institute of Technology, Newark, NJ, 2007

- Bachelor of Science in Mechanical Engineering,
  New Jersey Institute of Technology, Newark, NJ, 2002

Major: Mechanical Engineering

Publications:

Martin, P., Russell, K., and Sodhi, R. S., (Accepted For Publication), "On Mechanism Design Optimization For Motion Generation," Mechanism and Machine Theory, Elsevier Ltd.

To my beloved family & friends

ACKNOWLEDGMENT

The author would like to express his sincere gratitude to his advisor, Dr. Raj S. Sodhi for his guidance and support throughout the research. The author would also like to thank Dr. Ian S. Fischer and Dr. Kevin Russell for serving as committee members especially, Dr. Kevin Russell for all his support, encouragement and friendship. Without his countless hours of help this work would not have been able to be completed.

TABLE OF CONTENTS

LIST OF TABLES

LIST OF FIGURES

LIST OF FIGURES
(Continued)

LIST OF FIGURES
(Continued)

CHAPTER 1

INTRODUCTION

1.1 Background

Planar four-bar mechanisms are used in numerous mechanical systems. Due to the kinematic and design simplicity of planar four-bar mechanisms, they are typically very practical to design and incorporate in mechanical applications. The usefulness of these mechanisms is evident in applications ranging from simple tools and furniture (see Figure 1.1) to complex industrial machinery (see Figure 1.2). Extensive work on the design, analysis and synthesis of planar four-bar mechanisms has been introduced to date.

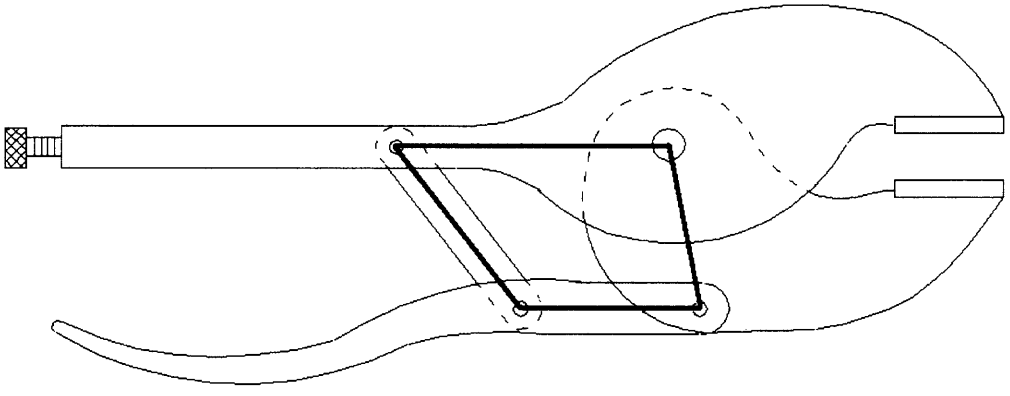

Figure 1.1 Four-bar mechanism application in simple hand tool.

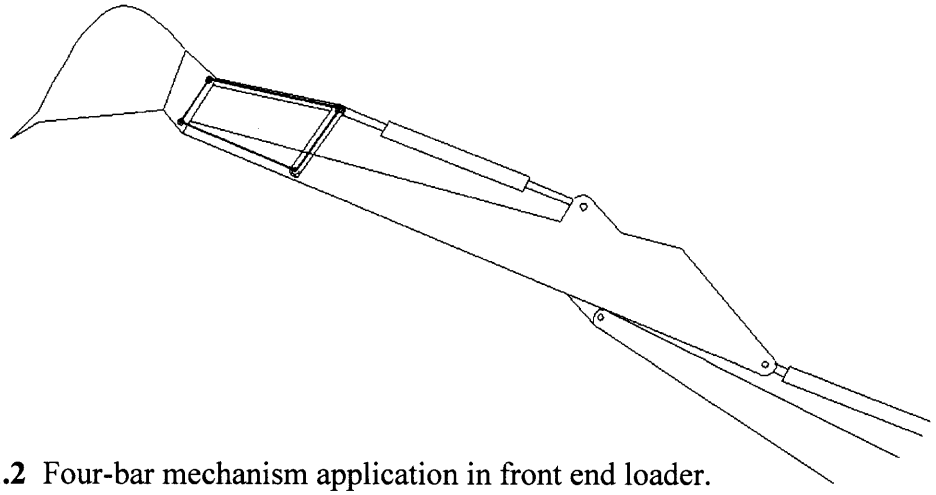

Figure 1.2 Four-bar mechanism application in front end loader.

Achieving specified rigid-body positions is often an important consideration when designing planar four-bar mechanisms. Kinematic motion generation involves the determination of particular mechanism variables required to approximate or precisely achieve particular user specified rigid-body positions. The planar four-bar mechanism variables typically include the fixed and moving pivot locations, the crank, follower and/or coupler orientations and lengths. Figure 1.3 illustrates one of the many common uses for a planar four-bar mechanism. The stamping link or the coupler in this four-bar mechanism moves through specific rigid body orientations to transfer the stamp from the ink pad to the box. If one only has information regarding the particular rigid-body positions required to stamp the ink pad and box, one could determine the mechanism parameters that would achieve the rigid-body positions through the use of a kinematic motion generation method.

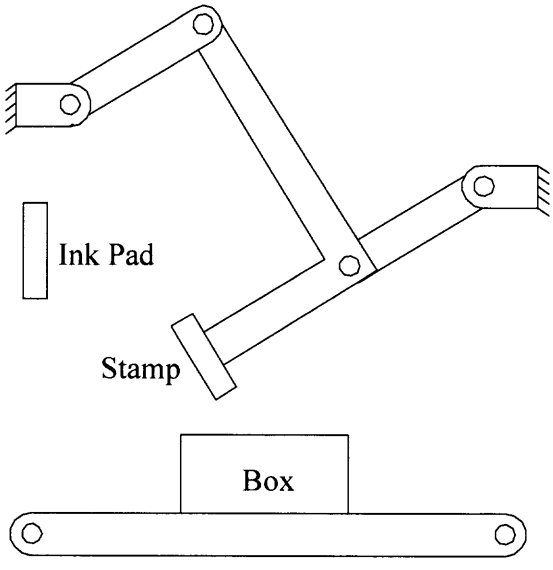

Figure 1.3 Planar four-bar stamping mechanism.

An analytical or graphical motion generation method such as Burmester curve synthesis or a numerical motion generation method can produce solution loci for the fixed and moving pivots for planar four-bar mechanisms. In Burmester curve synthesis, the solution loci are often called *circle point* and *center point* curves. These loci will be called *moving* and *fixed* pivot curves, respectively in this work. Although the fixed and moving pivot curves produced through Burmester curve synthesis and those generated through a numerical method require unique solution methodologies, both curves represent an infinite number of mechanical solutions for a series of prescribed rigid-body positions. From the fixed and moving pivot curves, the user can select an indefinite number of mechanism solutions. Although all of the mechanism solutions will achieve the prescribed rigid-body positions, some of them may not allow full crank rotatability, produce out-of-range transmission angles or not result in a compact four-bar mechanism design.

In order to efficiently and judiciously search a set fixed and moving pivot curves for an optimum mechanism solution, a search and selection methodology to narrow the indefinite number of mechanism solutions to determine the optimum solution (optimum with respect to specific design requirements and parameters) is required.

1.2 Literature Review

A great deal of research has been done in the field of mechanism synthesis and optimization both graphically and analytically. Previous work in the area of motion generation (rigid-body guidance) includes the work of Zhixing, Hongying, Dewei and Jiansheng [1] considered a guidance-line rotation method for the synthesis of planar

mechanism. Akhras and Angeles [2] presented an unconstrained nonlinear least-square techniques used in the optimization of planar mechanisms.

Previous work in the area of path generation includes the work of Vasiliu and Yannou [3] considered a method to synthesize the dimensions of a planar path generator mechanism by an approximating function which generates the trajectory shape. Sánchez Marín and González [4] considered a design method where space reduction is optimized in path synthesis mechanisms. Sancibrian, Viadero, García and Fernández [5] developed a gradient-based optimization approach for synthesis of planar path mechanisms. Tong and Chiang [6] produced the synthesis of planar and spherical four-bar path generators based on compatible equations from the geometrical relations between the pole of the coupler and the mechanism joints. Nolle and Hunt [7] presented a method in which analytical expressions are derived and the solution to these equations yields optimum synthesis of the planar four-bar coupler curve. Shi, Yang, Yang and Cheng [9] introduced a synthesis procedure which models the deviation of the actual path generated by a coupler point from the desired one.

Previous work in the area of function generation includes the work of Chiang [9] presented synthesis of four-bar function generators by means of equations of three relative poles, instead of the conventional four opposite relative poles. Rao [10] considered a geometric programming method to synthesis four-bar function generators. Alizade, Novruzbekov, and Sandor [11] introduced the optimal kinematic synthesis of mechanisms by application of the penalty function technique, and presents a new method of finding feasible initial approximations for the mechanism parameters. Bagci [12] presented a method of optimum synthesis of planar function generators, where the

dimensions of an optimum mechanism are determined by minimizing the error in Freudenstein's input-output displacement equation of the mechanism. Sandgren [13] developed a method for optimizing mechanisms by means of a nonlinear goal programming algorithm. Simionescu and Beale [14] presented an approach to optimum synthesis of the planar four-bar function generator using the Ackermann steering linkage considered as an example. Bagci and Rieser [15] considered a method of optimum synthesis of function generators mechanisms in which the derivatives of the generated displacements along with the displacements at a discrete set of design positions are satisfied.

Previous work in the area of synthesis and optimization for multiple mechanism types includes the work Cabrera, Simon and Prado [16] introduced solution methods for optimal synthesis of planar mechanisms by applying genetic algorithms based on evolutionary techniques and the type of goal function. Cossalter, Doria and Pasini [17] developed a numerical method to optimally synthesis planar mechanisms. Krishnamurty and Turcic [18] presented optimization techniques based on the methods of nonlinear goal programming to perform optimal synthesis of general planar mechanisms. Sutherland and Siddall [19] introduced a dimensional synthesis optimization method in which an objective function combining the contributions of kinematic structural error, mechanical error and link length to synthesis different types of mechanisms. Vallejo, Avilés, Hernández and Amezua [20] used a nonlinear optimization method to synthesis planar mechanisms of any type. Erdman [21] presented a method for the synthesis of planar linkages by means of modeling dyads by complex numbers in several different equation forms for three prescribed positions. Da Lio, Cossalter and Lot [22] introduced

the use of natural coordinates for the optimal synthesis of mechanisms. Sancibrian, García, Viadero and Fernández [23] developed a approach which uses exact differentiation to obtain gradient elements to the kinematic synthesis of path generation, function generation and rigid-body guidance in planar multibody systems. Fernández-Bustos, Aguirrebeitia, Avilés and Angulo [24] considered the use of genetic algorithms with a finite-element-based error function for kinematic analysis and synthesis of 1-dof mechanisms.

Other previous work in the area of mechanism synthesis and optimization includes the work Alba, Doblaré and Gracia [25] presented a method which minimizes the error between the actual path of one or several points of the mechanism and the paths for each of them predefined by a certain number of points for 2D and 3D mechanisms. Khare and Dave [26] introduced a method to optimize 4-bar crank-rocker mechanism by maximizing the minimum transmission angle. Lebedev [27] developed a vector method for the synthesis of planar mechanisms. Khare and Dave [28] described an analytical procedure for the synthesis of the planar four-bar double-rocker mechanism for optimum transmission characteristics. Sun and Waldron [29] developed graphical techniques which allow control of the maximum transmission angles in the design positions for mechanism synthesis. Waldron [30] presented a graphical iteration method for locating regions of the Burmester circle-point curve which give fully rotatable cranks. Chen [31] introduced a method for the synthesis of planar four-bar double-rocker mechanism by means of closed-form equations for determining the prescribed extreme positions.

1.3 Objectives and Scope of Work

In this work, algorithms for selecting planar four-bar motion generators with respect to Grashof conditions, mechanism perimeter constraints and transmission angle constraints are developed and presented. The algorithms search fixed and moving pivot curves and produce the parameters of the optimum motion generator (optimum with respect to particular Grashof conditions, transmission angle constraints and mechanism perimeter constraints). Two distinct algorithms have been developed and codified in MathCAD to support advanced analysis capabilities. One algorithm incorporates fixed and moving pivot curves generated by Burmester synthesis and the other incorporates numerically-generated fixed and moving pivot curves. Using these algorithms, the user can determine the parameters for planar four-bar mechanisms that not only achieve a series of user-prescribed rigid-body positions, but also satisfy Grashof constraints, minimum mechanism perimeter and transmission angle constraints.

CHAPTER 2

MOTION GENERATION

2.1 Burmester Curve Methodology

Planar four-bar mechanisms are sometimes depicted as two-link vector pairs called dyads. The dyads for a planar four-bar mechanism are illustrated in Figure 2.1. Vectors $\boldsymbol{W}$ and $\boldsymbol{Z}$ represent the left-side dyad of the four-bar mechanism and vectors $\boldsymbol{W}^*$ and $\boldsymbol{Z}^*$ represent the right-side dyad. Vectors $\boldsymbol{W}$ and $\boldsymbol{W}^*$ represent the crank and follower links, respectively. Variables $\boldsymbol{m}$ ($\boldsymbol{m}^*$), $\boldsymbol{k}$ ($\boldsymbol{k}^*$) and $\boldsymbol{P}$ represent the fixed pivots, moving pivots and coupler point, respectively.

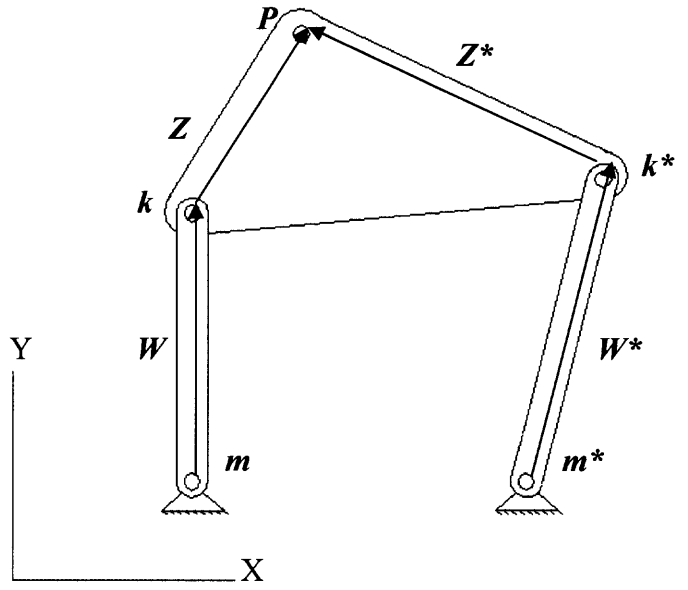

Figure 2.1 Planar four-bar mechanism dyads.

Figure 2.2 illustrates the left-side dyad in its initial position and its jth position in an arbitrary coordinate system. The locations of coupler point $\boldsymbol{P}$ in its initial position $\boldsymbol{P}_1$ and its jth position $\boldsymbol{P}_j$ are represented by vectors $\boldsymbol{R}_1$ and $\boldsymbol{R}_j$, respectively. The displacement of coupler point $\boldsymbol{P}$ from $\boldsymbol{P}_1$ to $\boldsymbol{P}_j$ is represented by a path displacement

vector δ_j where $\delta_j = R_j - R_1$. The angular displacement of the coupler link (the rotation of the Z vector from the initial position to the jth position) is represented by the variable α_j. The angular displacement of the crank link (the rotation of the W vector from the initial position to the jth position) is represented by the variable β_j.

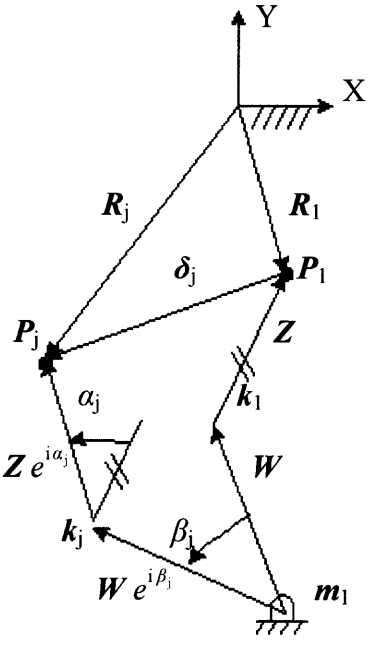

Figure 2.2 Left-side dyad in its first and jth position.

In motion generation, the initial position and configuration of the planar four-bar mechanism (and subsequently, the left and right-side dyad vectors) are unknown. To calculate vectors W and Z in Figure 2.2, Equation 2.2 is used. Equation 2.1 is the sum of the loop containing vectors W, Z and R_1 in the first and jth positions. Equation 2.2 is a rearranged expression of Equation 2.1 (where $\delta_j = R_j - R_1$ and vectors W and Z are factored out). Equation 2.2 is referred to as the "standard form."

Four prescribed coupler positions (i.e., j = 2, 3, 4) will result in the formation of three closed vector loops and subsequently, three standard form equations. Equations 2.3, 2.4 and 2.5 represent the standard forms for the dyad displacements from positions 1

to 2, 1 to 3 and 1 to 4, respectively. These three equations form a set of five unknowns ($\boldsymbol{W}, \boldsymbol{Z}, \beta_2, \beta_3, \beta_4$). User-prescribed variables include three coupler point displacements ($\boldsymbol{\delta}_j$) and three coupler displacement angles (α_j). For four prescribed positions one "free choice" is available to equate the number of unknowns to the number of equations. Table 2.1 depicts the possible number of unknowns and "free choices" for a given number of coupler positions. Assuming one has prescribed a range of angles β_2, a range of solutions for the six unknowns can be calculated using Equations 2.3, 2.4, and 2.5.

$$\boldsymbol{W}\, e^{i\beta_j} + \boldsymbol{Z}\, e^{i\alpha_j} - \boldsymbol{R}_j + \boldsymbol{R}_1 - \boldsymbol{Z} - \boldsymbol{W} = 0 \tag{2.1}$$

$$\boldsymbol{W}\left(e^{i\beta_j} - 1\right) + \boldsymbol{Z}\left(e^{i\alpha_j} - 1\right) = \boldsymbol{\delta}_j \tag{2.2}$$

$$\boldsymbol{W}\left(e^{i\beta_2} - 1\right) + \boldsymbol{Z}\left(e^{i\alpha_2} - 1\right) = \boldsymbol{\delta}_2 \tag{2.3}$$

$$\boldsymbol{W}\left(e^{i\beta_3} - 1\right) + \boldsymbol{Z}\left(e^{i\alpha_3} - 1\right) = \boldsymbol{\delta}_3 \tag{2.4}$$

$$\boldsymbol{W}\left(e^{i\beta_4} - 1\right) + \boldsymbol{Z}\left(e^{i\alpha_4} - 1\right) = \boldsymbol{\delta}_4 \tag{2.5}$$

Table 2.1 Maximum Number of Solutions for Unknown Dyad $\boldsymbol{W}$ (W_{Re}, W_{Im}), $\boldsymbol{Z}$ (Z_{Re}, Z_{Im}) when $\boldsymbol{\delta}_j$ and α_j are Prescribed

Number of coupler positions (j): j = 2, 3, ...,n	Number of equations	Number of unknowns	Number of free choices
2	2	5 ($\boldsymbol{W}, \boldsymbol{Z}, \beta_2$)	3
3	4	6 ($\boldsymbol{W}, \boldsymbol{Z}, \beta_2, \beta_3$)	2
4	6	7 ($\boldsymbol{W}, \boldsymbol{Z}, \beta_2, \beta_3, \beta_4$)	1
5	8	8 ($\boldsymbol{W}, \boldsymbol{Z}, \beta_2, \beta_3, \beta_4, \beta_5$)	0

Given any two of the three β values, Equations 2.2-2.5 can be solved for $\boldsymbol{Z}$ and $\boldsymbol{W}$ using Cramer's rule for example. If one selects a range of β_2 values, a locus of moving pivot locations (variable $\boldsymbol{k}_1$ in Figure 2.2) could be produced knowing $\boldsymbol{k}_1 = \boldsymbol{R}_1 - \boldsymbol{Z}$ and a locus of the fixed pivot locations (variable $\boldsymbol{m}_1$ in Figure 2.2) could be produced knowing $\boldsymbol{m} = \boldsymbol{k}_1 - \boldsymbol{W}$. Fixed and moving pivot curves are also called circle and center point curves,

respectively, or more commonly, *Burmester curves*. Figure 2.3 illustrates a pair of Burmester curves produced for four prescribed coupler positions. Each point on the moving pivot curve has a corresponding fixed pivot curve point (or vice-versa). A planar four-bar motion generator can be constructed given two pairs of moving and fixed pivot curve points (see Figure 2.3).

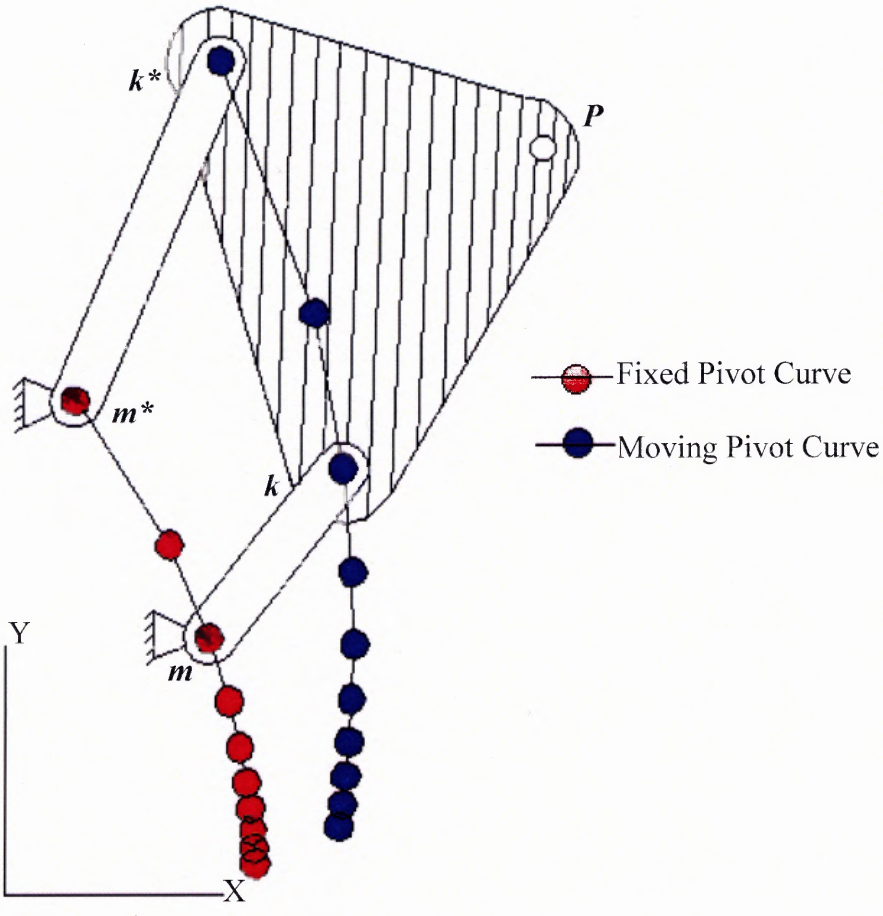

Figure 2.3 Burmester curve pair.

2.2 Burmester Curve Algorithm

As mentioned in the Section 2.1, it was assumed that ranges for angles β_3 and β_4 could be determined given a prescribed range for angle β_2. Equations 2.3 through 2.5 are represented in matrix form in Equation 2.6. The second column of the coefficient matrix

in Equation 2.6 and the right side column matrix contain the prescribed data and the first column of the coefficient matrix contains the unknown displacement angles β_3 and β_4. The solution to the system will only exist if the rank of the augmented matrix of the coefficients is 2. The augmented matrix $\boldsymbol{M}$ in Equation 2.7 is formed by adding the right side column and left side coefficient matrices in Equation 2.6. If the rank of the augmented matrix is 2, its determinant is zero (Equations 2.7 and 2.8).

$$\begin{bmatrix} e^{i\beta_2}-1 & e^{i\alpha_2}-1 \\ e^{i\beta_3}-1 & e^{i\alpha_3}-1 \\ e^{i\beta_4}-1 & e^{i\alpha_4}-1 \end{bmatrix} \begin{bmatrix} \boldsymbol{W} \\ \boldsymbol{Z} \end{bmatrix} = \begin{bmatrix} \boldsymbol{\delta}_2 \\ \boldsymbol{\delta}_3 \\ \boldsymbol{\delta}_4 \end{bmatrix} \tag{2.6}$$

$$\mathrm{Det}[\boldsymbol{M}] = \mathrm{Det} \begin{bmatrix} e^{i\beta_2}-1 & e^{i\alpha_2}-1 & \boldsymbol{\delta}_2 \\ e^{i\beta_3}-1 & e^{i\alpha_3}-1 & \boldsymbol{\delta}_3 \\ e^{i\beta_4}-1 & e^{i\alpha_4}-1 & \boldsymbol{\delta}_4 \end{bmatrix} = 0 \tag{2.7}$$

Since the unknowns in Equation 2.7 are in the first column of the augment matrix $\boldsymbol{M}$, the determinant can be expanded about this column (see Equation 2.8). The Δ variables represent the cofactors of the elements in the first column of Equation 2.7. In Equations 2.9 through 2.12, the Δ variables are known since they contain only known input data.

$$\Delta_2 e^{i\beta_2} + \Delta_3 e^{i\beta_3} + \Delta_4 e^{i\beta_4} + \Delta_1 = 0 \tag{2.8}$$

where

$$\Delta_1 = -\Delta_2 - \Delta_3 - \Delta_4 \tag{2.9}$$

$$\Delta_2 = \begin{vmatrix} e^{i\alpha_3}-1 & \boldsymbol{\delta}_3 \\ e^{i\alpha_4}-1 & \boldsymbol{\delta}_4 \end{vmatrix} \tag{2.10}$$

$$\Delta_3 = \begin{vmatrix} e^{i\alpha_2}-1 & \boldsymbol{\delta}_2 \\ e^{i\alpha_4}-1 & \boldsymbol{\delta}_4 \end{vmatrix} \tag{2.11}$$

$$\Delta_4 = \begin{vmatrix} e^{i\alpha_2} - 1 & \delta_2 \\ e^{i\alpha_3} - 1 & \delta_3 \end{vmatrix} \tag{2.12}$$

In Equation 2.8 (also referred to as the compatibility equation), the unknowns variables are the exponents β_2, β_3 and β_4. Given a value or a range of values for β_2, a solution or range of solutions for variables β_3 and β_4 in Equation 2.8 can be determined either geometrically (see Figure 2.4) or calculated using the algorithm given in Equations 2.15 through 2.24 [32]. Equation 2.8 can be further simplified into Equation 2.13.

$$\Delta_3 e^{i\beta_3} + \Delta_4 e^{i\beta_4} = -\Delta \tag{2.13}$$

where

$$-\Delta = -\Delta_1 - \Delta_2 e^{i\beta_2} \tag{2.14}$$

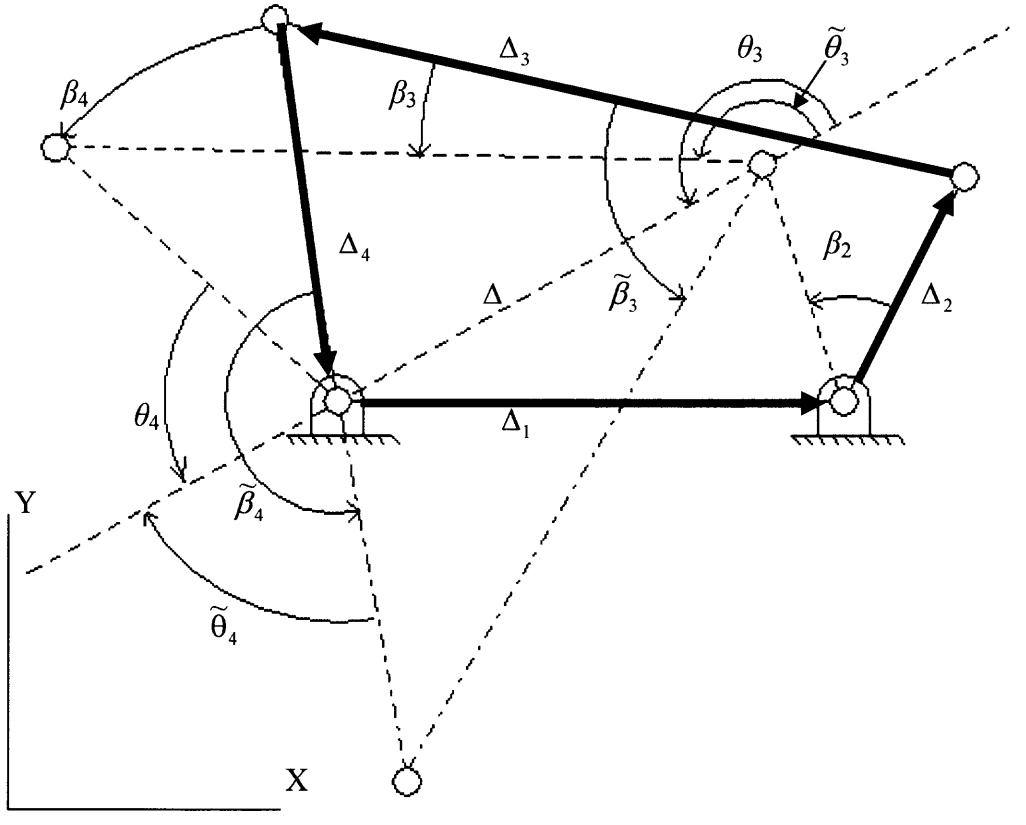

Figure 2.4 Geometric solution of Equations 2.2-2.5 for the unknown angles β_j.

$$\Delta = \Delta_1 + \Delta_2 e^{i\beta_2} \tag{2.15}$$

$$\cos\theta_3 = \frac{|\Delta_4|^2 - |\Delta_3|^2 - |\Delta|^2}{2|\Delta_3||\Delta|} \tag{2.16}$$

$$\sin\theta_3 = \left|\sqrt{(1-\cos^2\theta_3)}\right| \geq 0 \text{ where } 0 \leq \theta_3 \leq \pi \tag{2.17}$$

$$\beta_3 = \arg\Delta + \theta_3 - \arg\Delta_3 \tag{2.18}$$

$$\widetilde{\theta}_3 = 2\pi - \theta_3 \tag{2.19}$$

$$\widetilde{\beta}_3 = \arg\Delta + \widetilde{\theta}_3 - \arg\Delta_3 \tag{2.20}$$

$$\cos\theta_4 = \frac{|\Delta_3|^2 - |\Delta_4|^2 - |\Delta|^2}{2|\Delta_4||\Delta|} \tag{2.21}$$

$$\sin\theta_4 = \left|\sqrt{(1-\cos^2\theta_4)}\right| \geq 0 \text{ where } 0 \leq \theta_4 \leq \pi \tag{2.22}$$

$$\beta_4 = \arg\Delta + \theta_4 - \arg\Delta_4 \tag{2.23}$$

$$\widetilde{\beta}_4 = \arg\Delta + \theta_4 - \arg\Delta_4 + \pi \tag{2.24}$$

2.3 Numerical Motion Generation

Figure 2.5 illustrates a planar four-bar mechanism. In this work, link ***m-k*** is designated as the input (or crank) while link $\boldsymbol{m}^*$-$\boldsymbol{k}^*$ is designated as the output (or follower) link. The lengths of ***m-k*** and $\boldsymbol{m}^*$-$\boldsymbol{k}^*$ are represented by R_1 and R_2, respectively. The crank and follower links of the planar four-bar motion generator must satisfy a constant length condition only. Given a general fixed pivot ***m*** and a moving pivot ***k***, the constant length condition in Equation 2.25 must be satisfied when synthesizing the crank and follower links of the planar four-bar motion generator.

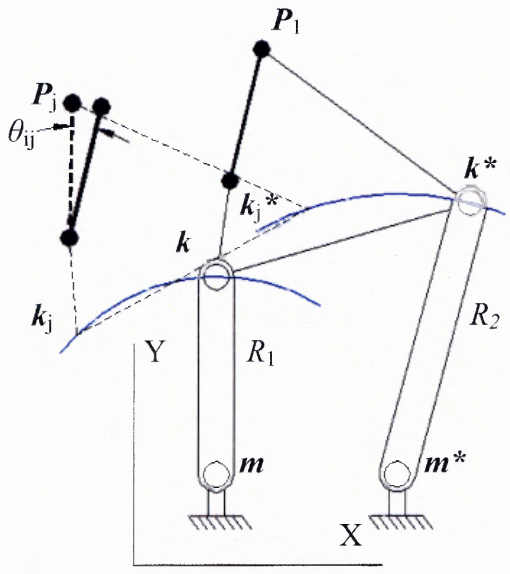

Figure 2.5 Four-bar motion generator with coupler point $\boldsymbol{P}$ and orientation angle θ.

$$(\boldsymbol{k}_j - \boldsymbol{m})^T(\boldsymbol{k}_j - \boldsymbol{m}) = (\boldsymbol{k} - \boldsymbol{m})^T(\boldsymbol{k} - \boldsymbol{m}) \quad j = 2, 3, \ldots n \tag{2.25}$$

where

$$\boldsymbol{k} = (k_x, k_y, 1), \qquad \boldsymbol{m} = (m_x, m_y, 1), \qquad \boldsymbol{m}_j = [D_{1j}]\boldsymbol{m}$$

and

$$[D_{1j}] = \begin{bmatrix} \cos\theta_{1j} & -\sin\theta_{1j} & p_{jx} - p_{1x}\cos\theta_{1j} + p_{1y}\sin\theta_{1j} \\ \sin\theta_{1j} & \cos\theta_{1j} & p_{jy} - p_{1x}\sin\theta_{1j} - p_{1y}\cos\theta_{1j} \\ 0 & 0 & 1 \end{bmatrix} \tag{2.26}$$

Equation 2.25 is rewritten as Equation 2.27. In Equation 2.27, the variable R represents the length of the link.

$$(\boldsymbol{k}_j - \boldsymbol{m})^T(\boldsymbol{k}_j - \boldsymbol{m}) = R^2 \quad j = 2, 3, \ldots n \tag{2.27}$$

Equation 2.26 represents the displacement of the coupler from the initial position to the jth position. The variable $\boldsymbol{P}$ represents the position of a coupler curve point while variable θ represents the angular displacement of the coupler between the initial position and jth position. Since there are five variables (k_x, k_y, m_x, m_y and R), a maximum of six

coupler positions can be chosen, with no arbitrary choice of parameter. Given five prescribed rigid-body positions, Equations 2.28 through 2.31 can be used with one arbitrary choice of parameter.

$$(\boldsymbol{k}_2 - \boldsymbol{m})^{\mathrm{T}}(\boldsymbol{k}_2 - \boldsymbol{m}) - R^2 = 0 \tag{2.28}$$

$$(\boldsymbol{k}_3 - \boldsymbol{m})^{\mathrm{T}}(\boldsymbol{k}_3 - \boldsymbol{m}) - R^2 = 0 \tag{2.29}$$

$$(\boldsymbol{k}_4 - \boldsymbol{m})^{\mathrm{T}}(\boldsymbol{k}_4 - \boldsymbol{m}) - R^2 = 0 \tag{2.30}$$

$$(\boldsymbol{k}_5 - \boldsymbol{m})^{\mathrm{T}}(\boldsymbol{k}_5 - \boldsymbol{m}) - R^2 = 0 \tag{2.31}$$

Equations 2.28 through 2.31 form a set of four non-linear simultaneous equations and can be solved numerically using Newton's method for example. With Newton's method, initial guesses of the unknown variables to be determined are required. The use of Computer-Aided Design software could enable one to make judicious initial guesses for the unknown variables. Since only one of the five unknown variables can be specified, the user is free to specify a single value or a range of values. Assuming the latter, a range of solutions corresponding to the range for the specified variable is calculated. For example, the user can specify a range for variable m_x and calculate m_y, k_x, k_y and R for each value of m_x specified in the range. The end results are ranges of solutions for the unknown variables.

Given the solution ranges for m_x and m_y, a fixed pivot curve is formed while the solution ranges for k_x and k_y form a moving pivot curve. Figure 2.6 illustrates fixed and moving pivot curves produced for five prescribed coupler positions using the approach described in the previous paragraph. Each point on the fixed pivot curve has a corresponding point on the moving pivot curve (or vice-versa). A planar four-bar motion generator can be constructed given two pairs of fixed and moving point curve points and

is illustrated in Figure 2.6. These numerically produced fixed and moving pivot loci are analogous to Burmester center point and circle point curves, respectively [32].

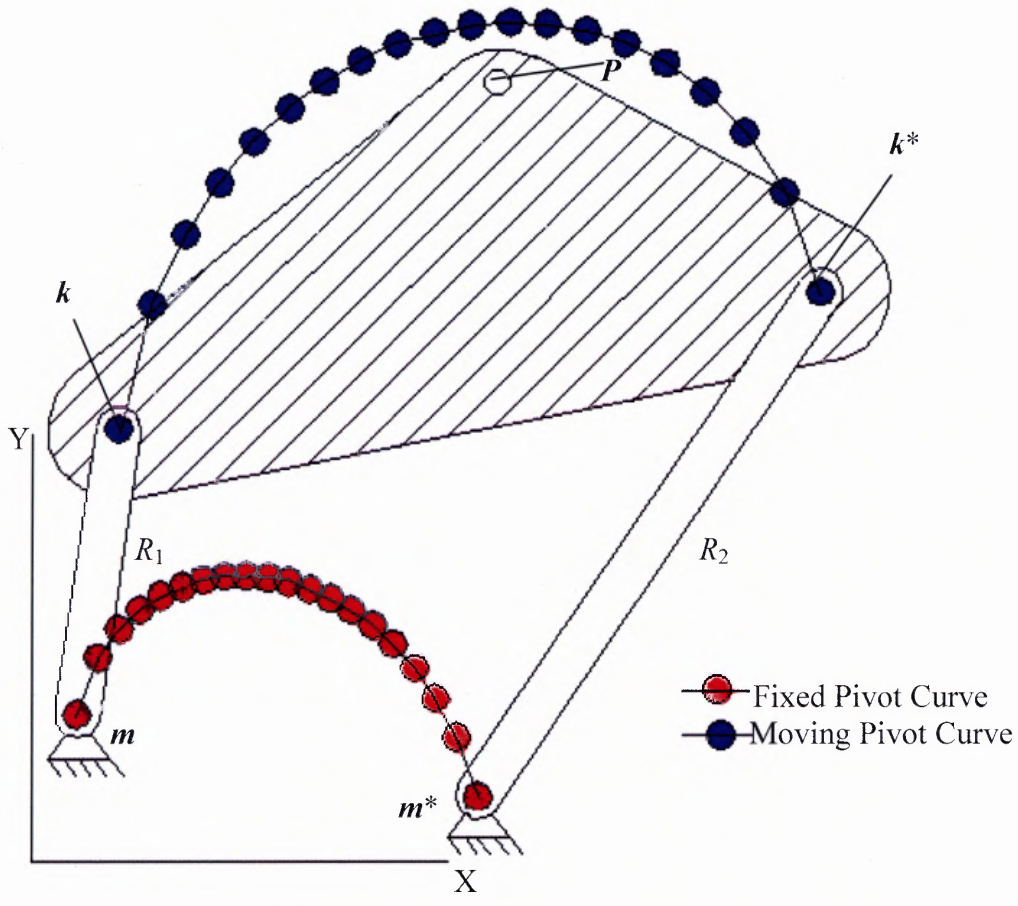

Figure 2.6 Fixed and moving pivot curves.

CHAPTER 3

MECHANISM SELECTION CRITERIA AND ALGORITHMS

3.1 Mechanism Selection Criteria

A planar four-bar mechanism design with complete crank rotatability is often necessary. For example, when a drive mechanism is implemented to rotate the crank link continuously, full crank rotatability is a requirement. A planar four-bar mechanism in which one of the links can perform a full rotation relative to the other three links is classified as a Grashof mechanism. Grashof criteria predict link rotatability and are based on the lengths of the four links as well as the inversions of the four-bar linkage. Five classifications for planar four-bar Grashof mechanisms exist and are given in Table 3.1. In Table 3.1, variables, L_{min}, L_{max}, L_a and L_b represent the longest link length, shortest link length, and intermediate link lengths, respectively. With the exception of the Grashof Triple Rocker (also called a Non-Grashof mechanism), all Grashof mechanisms have at least one fully rotatable link.

Table 3.1 Classification of Planar Four-bar Grashof Mechanisms

Type of Mechanism	Shortest Link	Relationship between Link Lengths
Crank rocker	Crank	$L_{max} + L_{min} < L_a + L_b$
Drag link	Ground	$L_{max} + L_{min} < L_a + L_b$
Double rocker	Coupler	$L_{max} + L_{min} < L_a + L_b$
Change point	Any	$L_{max} + L_{min} = L_a + L_b$
Triple rocker	Any	$L_{max} + L_{min} > L_a + L_b$

The Grashof inequalities are based on basic geometric triangle principles [33]. Figure 3.1 and Figure 3.2 represent two limiting positions of a crank-rocker mechanism. By applying basic geometric principles to Figure 3.1 and Figure 3.2, Equations 2.27-2.32

can be derived from the fundamental principle that the length of one side of a triangle (hypotenuse) must be less than the sum of the lengths of the other two sides.

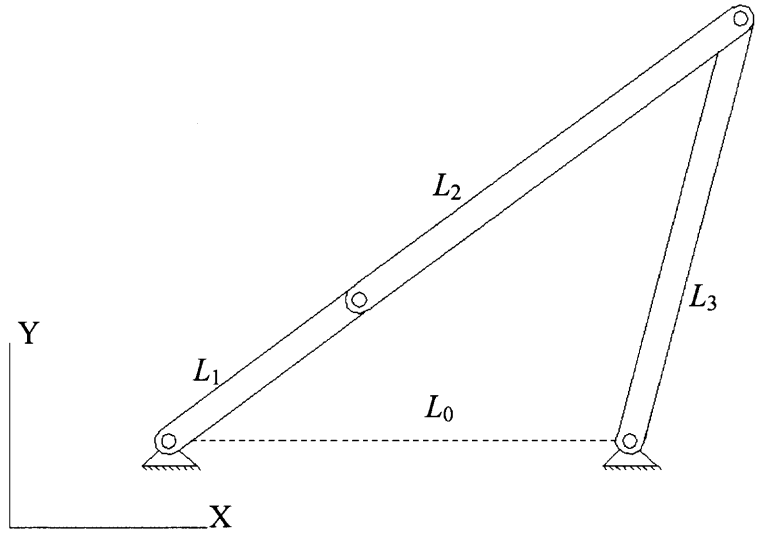

Figure 3.1 Limiting position of a crank-rocker mechanism.

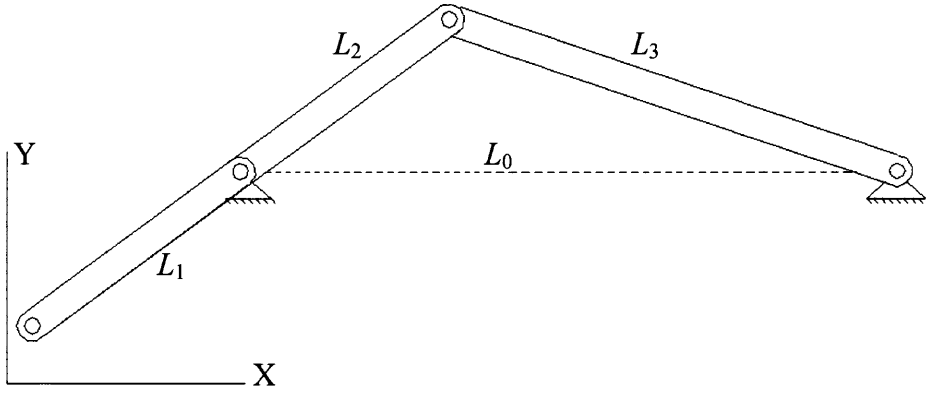

Figure 3.2 Limiting position of a crank-rocker mechanism.

$$L_0 < L_2 - L_1 + L_3 \tag{3.1}$$

$$L_2 - L_1 < L_3 + L_0 \tag{3.2}$$

$$L_3 < L_0 + L_2 - L_1 \tag{3.3}$$

$$L_0 < L_1 + L_2 + L_3 \tag{3.4}$$

$$L_1 + L_2 < L_0 + L_3 \tag{3.5}$$

$$L_3 < L_0 + L_1 + L_2 \tag{3.6}$$

Adding Equations 3.1 and 3.3 results in Equation 3.7.

$$L_0 + L_3 < L_2 - L_1 + L_3 + L_0 + L_2 - L_1 \tag{3.7}$$

where

$$0 < 2L_2 - 2L_1 \tag{3.8}$$

or

$$L_1 < L_2 \tag{3.9}$$

Similarly, combining Equations 3.1 and 3.5 results in Equation 3.10

$$L_1 < L_3 \tag{3.10}$$

and combining Equations 3.3 and 3.5 results in Equation 3.11

$$L_1 < L_0 \tag{3.11}$$

Therefore the crank must be the shortest link in the four-bar mechanism. If the fixed link or ground link is the longest link in Equation 3.1 then the Grashof criteria in Equation 3.12 results.

$$L_{max} + L_{min} < L_a + L_b \tag{3.12}$$

For all possible inversions of the crank rocker mechanism Equation 3.12 holds true. Incorporating Grashof criteria into a fixed and moving pivot curve search algorithm will enable one to design motion generators of any Grashof mechanism classification.

Another practical characteristic in the design of planar four-bar mechanisms is that it is compact. In this work, a compact mechanism is defined as one in which the sum of the lengths of the four linkages (crank, coupler, follower and ground) or *mechanism*

perimeter is the smallest possible (see Figure 3.3). As seen in Figure 3.3, for the same point of interest ***P***, the perimeter of mechanism 1 is smaller than mechanism 2. A compact mechanism generally requires less material, produces smaller workspaces, is more structurally sound (resulting in greater load-carrying capacity) and generates larger transmission angles (resulting in reduced joint wear) than non compact mechanisms.

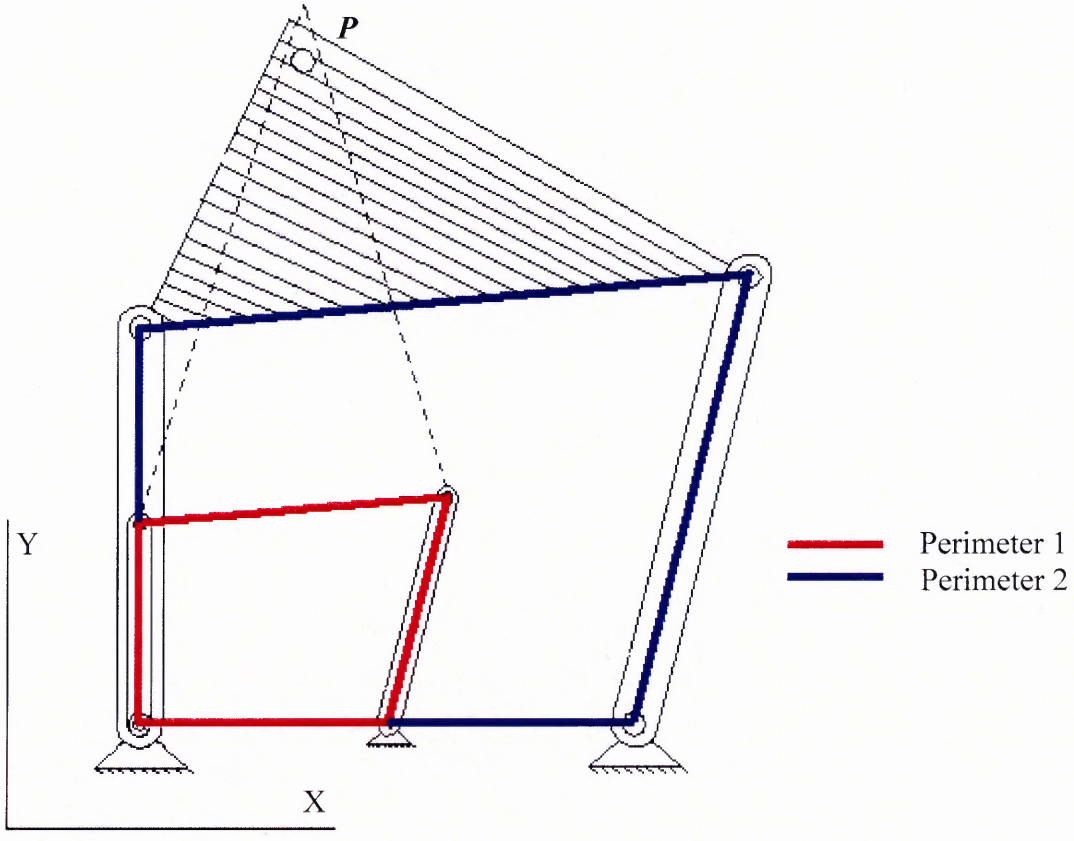

Figure 3.3 Planar four-bar compact mechanism.

The transmission angle (angle ϕ in Figure 3.4) is the angle between the coupler and the follower or output link. Transmission angles are optimally no less than 40° or 45° and no greater than 135° or 140° depending on the design of the joint and lubrication [32]. Figure 3.4 illustrates a mechanism with an extreme transmission angle. As link 1 rotates and the transmission angle reaches extreme values the torque force transmitted

from link 2 to link 3 is at its lowest but joint 1 sees high load bearing forces causing excessive wear or mechanism failure. When the load bearing forces exceed the transmitted torque the mechanism will lock and possibly break. The links in Figure 3.5 form a quadrilateral where the length of the diagonal is represented by variable L_d. Equation 3.13 is formed using the law of cosines for the triangle formed by L_1, L_2 and L_d.

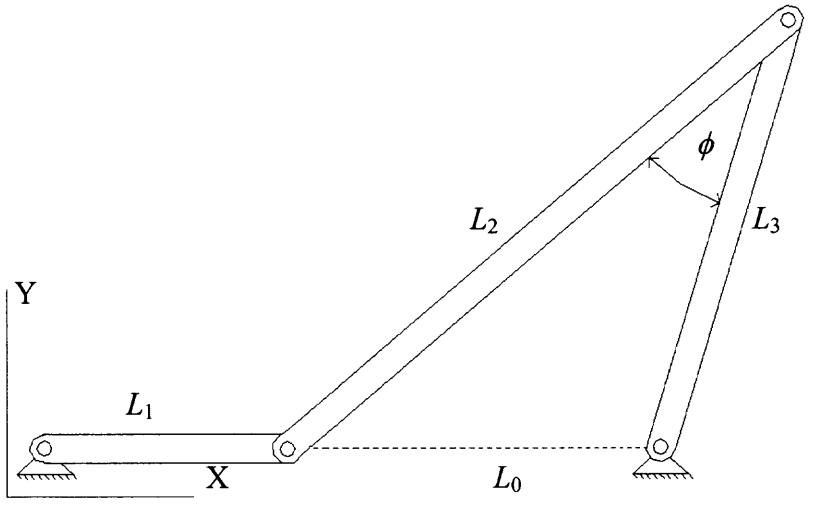

Figure 3.4 Planar four-bar mechanism with extreme transmission angle.

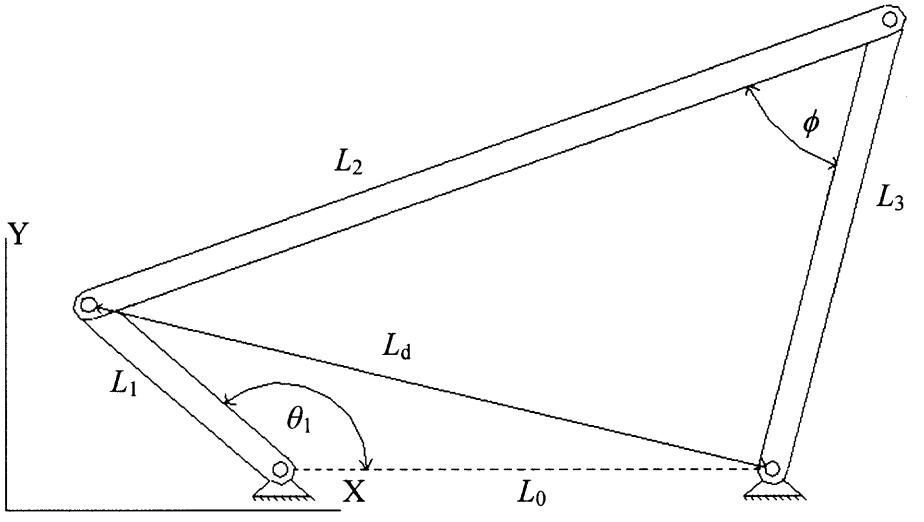

Figure 3.5 Planar four-bar mechanism breakdown to determine transmission angle.

$$L_d^2 = L_0^2 + L_1^2 - 2 L_0 L_1 \cos\theta_1 \tag{3.13}$$

Using the triangle L_3, L_2 and L_d and the law of cosines result in Equations 3.14 and 3.15.

$$L_d^2 = L_2^2 + L_3^2 - 2 L_2 L_3 \cos\phi \tag{3.14}$$

or

$$\cos\phi = \frac{L_2^2 + L_3^2 - L_d^2}{2 L_2 L_3} \tag{3.15}$$

Using Equation 3.15 the transmission angle at any instance can be calculated. The positions of interest are the two extreme positions (when the crank link and ground link are colinear) of the mechanism. The maximum and minimum transmission angles occur at these positions.

3.2 Optimum Mechanism Selection Algorithms

Figure 3.6 illustrates a diagram of the two algorithms developed in this work. Fixed and moving-pivot curves generated either by Burmester approach or numerically are the initial input the dimensional parameters and operational parameters of the optimized motion generator are the final output. Although both algorithms share common procedures in blocks 2 through 4 in Figure 3.6, this section will explain the distinctions in blocks 1 and 5 between both algorithms.

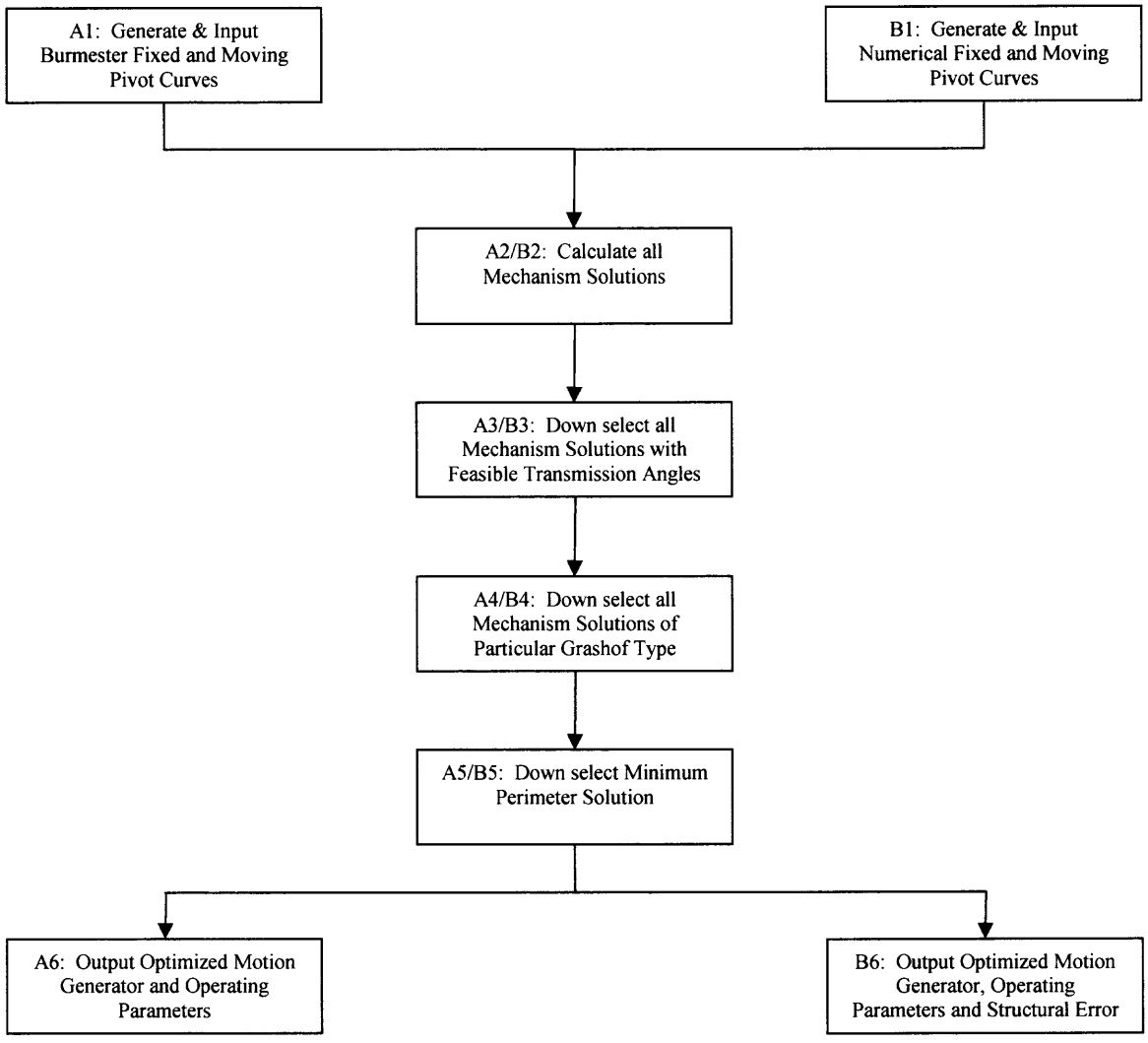

Figure 3.6 Flow chart of mechanism design algorithms.

The first procedure in the algorithms (blocks A1 and B1 in Figure 3.6) involves the calculation of fixed and moving pivot curves for a series of prescribed rigid-body positions. In block B1, the fixed and moving pivot curves are calculated numerically using the method described in Section 2.3. In block A1, the fixed and moving point curves are calculated algebraically using the Burmester algorithm given in Section 2.2. Although fixed and moving pivot curves generated by the Burmester algorithm and those generated numerically are calculated using unique quantitative methods, they all support the concept that there is an indefinite number of mechanism solutions for a series of four

or five rigid-body positions. In blocks A1 and B1, four rigid-body displacements represented by five distinct rigid-body positions and associated coupler displacement angles are prescribed. The type of Grashof mechanism (i.e., crank rocker, double rocker, etc) solution desired is also selected. The MathCAD code associated with blocks A1 and B1 can be seen in Appendix A (Section 1) and B (Section 1), respectively.

The second procedure in the algorithms (block 2 in Figure 3.6) involves the calculation of every possible mechanism solution for the prescribed rigid-body positions. These solutions include the lengths of the crank, coupler follower and ground links of each planar four-bar motion generator. By measuring the distances between all combinations of any two moving and fixed point curve sets the link lengths of every mechanism solution were calculated. In the example problems in this work, these mechanism solutions are illustrated as line and surface plots. The MathCAD code associated with blocks A2/B2 can be seen in Appendix A (Section 2) and B (Section 2), respectively.

The third procedure in the algorithm (block 3 in Figure 3.6) involves the calculation and selection of all mechanism solutions (from the solutions calculated in the second procedures) that do not violate the user-prescribed minimum and maximum transmission angle constraints. In block A3/B3, the transmission angles are calculated over a user-prescribed crank angle range for every possible mechanism solution in the second procedure. The MathCAD code associated with blocks A3/B3 can be seen in Appendix A (Section 3) and B (Section 3), respectively.

The fourth procedure in the algorithm (block 4 in Figure 3.6) involves the selection of all mechanism solutions of a particular Grashof classification from among the possible solutions produced in the third procedure. The user specifies the particular Grashof mechanism solution to be determined. Table 1 in Chapter 2 includes all of the Grashof mechanism classifications and conditions. The MathCAD code associated with blocks A4/B4 can be seen in Appendix A (Section 4) and B (Section 4), respectively.

The fifth procedure in the algorithm (block 5 in Figure 3.6.) involves the selection of the mechanism solution from among the possible solutions produced in the fourth procedure with the smallest perimeter. A minimum perimeter condition will ensure the selection of the most compact four-bar motion generator design. In general, compact mechanisms produce smaller workspaces, are more structurally sound and generates larger transmission angles than four-bar mechanisms with larger perimeters. The MathCAD code associated with blocks A5/B5 can be seen in Appendix A (Section 5) and B (Section 5), respectively.

The sixth procedure in the algorithm (blocks A6 and B6 in Figure 3.6) involves the calculation of the dimensional parameters of the most compact Grashof motion generator produced in the fifth procedure. These parameters include the fixed and moving pivot coordinates and the driving link angles required to achieve the prescribed rigid body positions. In block B6, the crank displacement angles required to approximate the prescribed rigid body positions with minimum structural error are calculated. Since the fixed and moving loci are calculated numerically in block B1, a degree of structural error will exist in the mechanism solution between the prescribed rigid body positions and the closest approximation achieved by the synthesized motion generator. In block

A6, the crank displacement angles required to achieve the prescribed rigid body positions are calculated. Since the fixed and moving pivot curves calculated by the Burmester algorithm are calculated algebraically (unlike the fixed and moving pivot loci in block B1) in block A1, no structural is associated with its mechanism solution. The MathCAD code associated with blocks A6 and B6 can be seen in Appendix A (Section 6) and B (Section 6), respectively.

CHAPTER 4

EXAMPLE PROBLEMS

4.1 Optimized Grashof Crank-Rocker Motion Generator

This example demonstrates the synthesis of a Grashof crank-rocker motion generator with minimum perimeter and feasible transmission angles ($40° \leq \phi \leq 140°$) given a series of prescribed rigid-body positions.

Table 4.1 includes the prescribed point coordinates and displacement angles for four rigid-body positions. Given these rigid-body positions, fixed and moving pivot curves will be produced using the Burmester method described in Section 2.2 (Block A1 in Figure 3.6 and Appendix A Section 1.1). Using the following range for variable β_2:

$$\beta_2 = 0.05, 0.1 \ldots 0.75 \text{ rad}$$

the fixed and moving pivot curves illustrated in Figure 4.1 are produced. As the prescribed increment for β_2 decreases the number on data points for the fixed and moving pivot curves and subsequently, the number of available four-bar motion generator solutions increases.

Table 4.1 Prescribed Rigid-body Parameters

Rigid-Body Positions			
	P	$\theta°$	$\alpha°$
1	1.4159, 1.9161	0	0
2	1.6345, 1.7778	3.6292	3.6292
3	1.6356, 1.6369	13.5386	13.5386
4	0.8147, 1.4919	51.8900	51.8900

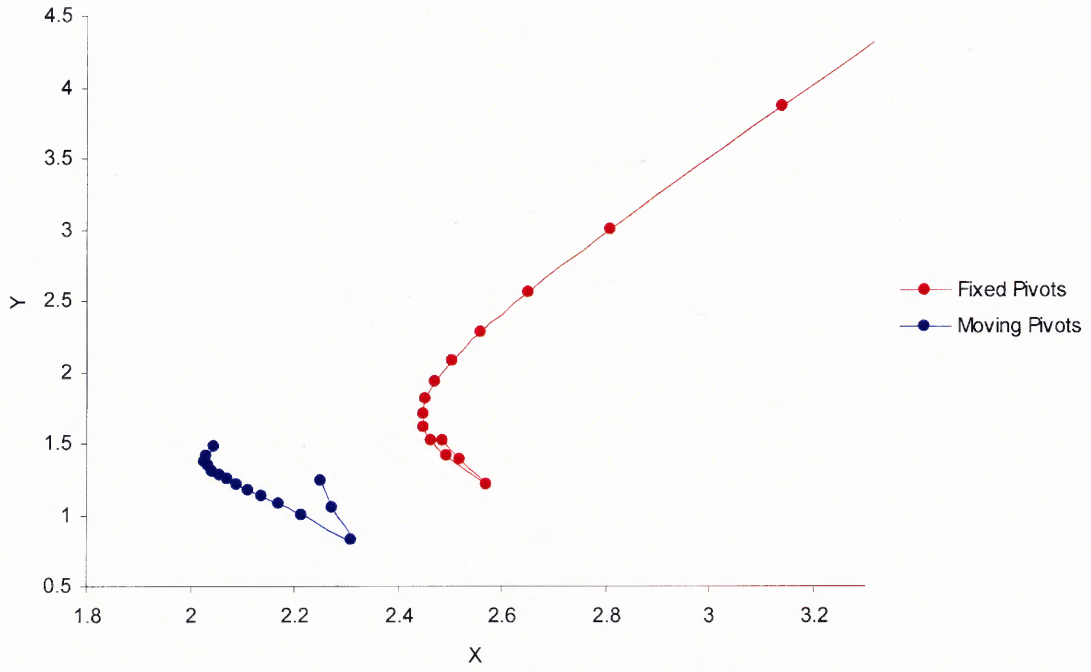

Figure 4.1 Fixed and moving pivot curves generated from data in Table 4.1.

From the output of Appendix A Section 1.2 (Block A2 in Figure 3.6), a plot of the crank/follower lengths of every four-bar motion generator solution in the fixed and moving pivot curves in Figure 4.1 is produced and illustrated in Figure 4.2. The abscissa in Figure 4.2 represents the sequentially assigned data point number and the ordinate represents the crank/follower length. The crank/follower length is the distance between each fixed pivot point and the corresponding moving pivot point.

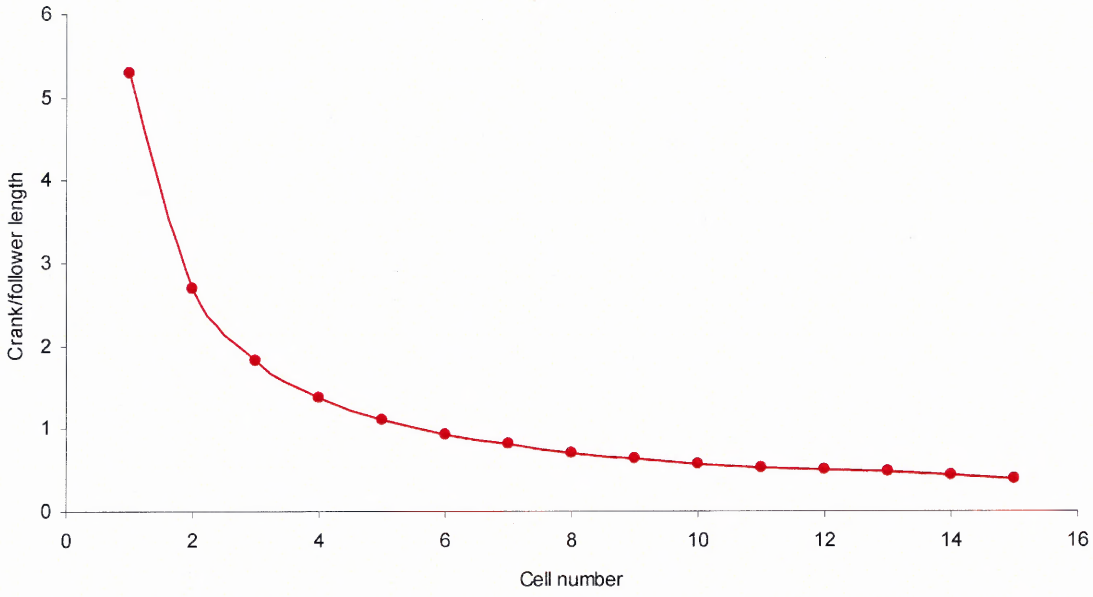

Figure 4.2 Crank/follower length solutions from fixed and moving pivot curves in Figure 4.1.

From the output of Appendix A Section 1.2 (Block A2 in Figure 3.6), surface plots of the coupler and ground lengths of every four-bar motion generator solution in the fixed and moving pivot curves in Figure 4.1 is produced and illustrated in Figure 4.3 and Figure 4.4, respectively. The horizontal and vertical axes in Figure 4.3 and Figure 4.4 are identical and represent the sequentially assigned data point number and the axis normal to the page represents the coupler length in Figure 4.3 and the ground length in Figure 4.4. The crank/follower length is the distance between each fixed pivot point and the corresponding moving pivot point. The coupler length is the distance between any two moving pivot points and the ground length is the distance between any two fixed pivot points.

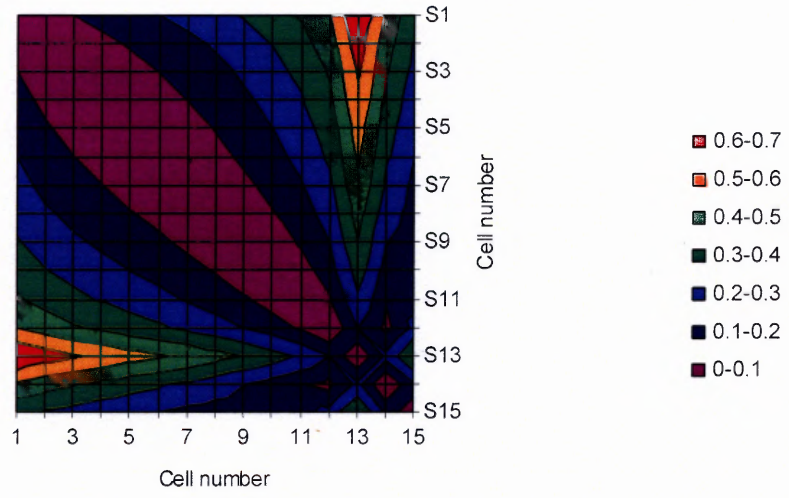

Figure 4.3 Coupler length solutions from fixed and moving pivot curves in Figure 4.1.

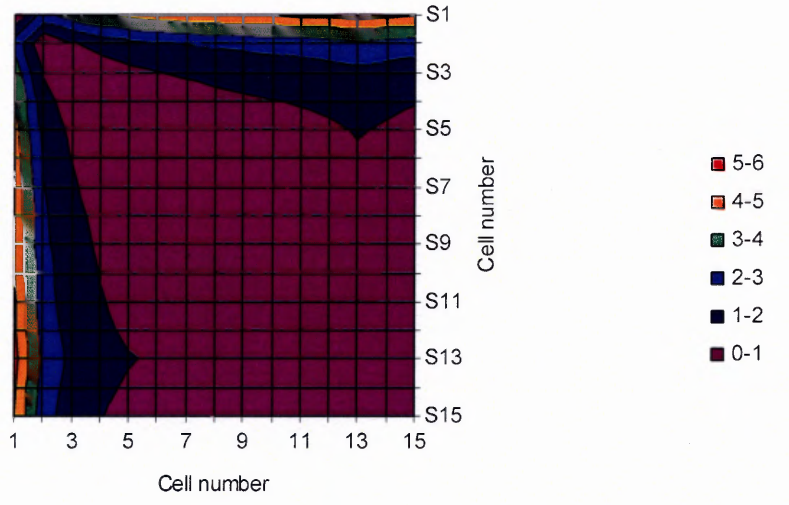

Figure 4.4 Ground length solutions from fixed and moving pivot curves in Figure 4.1.

Given such a potentially vast number of mechanism solutions, the Burmester curve-based optimization algorithm presented in this work enables one to select an optimum motion generator solution with respect to Grashof criteria, mechanism perimeter and transmission angle criteria judiciously and efficiently.

After the transmission angle calculation stage and the down selection stages (Block A3 in Figure 3.6 and Appendix A Section 1.3), the fixed pivots, moving pivots and crank displacement angles for the optimized motion generator selected are produced

in block A6 (Appendix A Section 1.6). The following are the fixed pivots, moving pivots and crank displacement angles for the optimized motion generator selected:

$\boldsymbol{m}$ = (2.5693, 1.2089), $\boldsymbol{k}$ = (2.3082, 0.8245), $\boldsymbol{m}^*$ = (3.1379, 3.8533), $\boldsymbol{k}^*$ = (2.0298, 1.4117)

The displacement angles (rad) are required to achieve the prescribed rigid-body positions.

$$\beta_2 = 0.6500, \beta_3 = 1.0162, \beta_4 = 4.2538$$

The crank link (link ***m-k***) has a length of 0.4647 units (therefore L_{min} = crank = 0.4647). The ground link (L_{max}) has a length of 2.7048 units. The sum of the remaining two links (the follower link and coupler link) is 3.3312 units. According to Grashof criteria in Table 3.1, the optimized mechanism is indeed a crank-rocker.

Figure 4.5 illustrates the optimized Grashof crank-rocker motion generator. The graph in Figure 4.6 illustrates the transmission angles produced by the optimized Grashof Crank-rocker motion generator. Figure 4.6 shows the transmission angle achieved by the synthesized motion generator in Figure 4.5 and are within the min/max transmission angle criteria ($40° \leq \phi \leq 140°$)

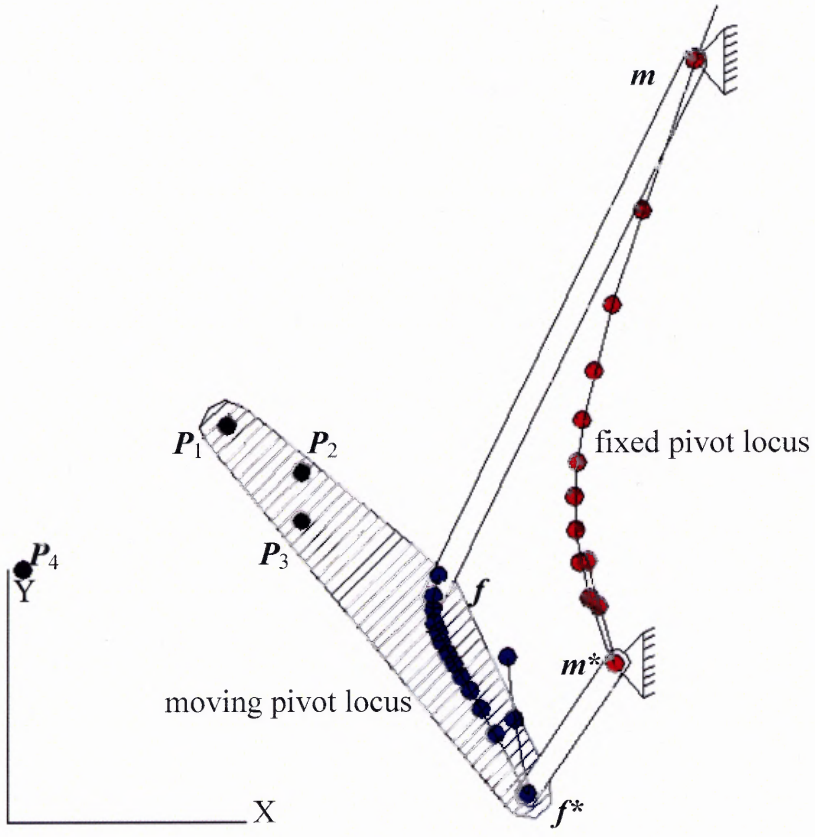

Figure 4.5 Optimized Grashof crank-rocker motion generator.

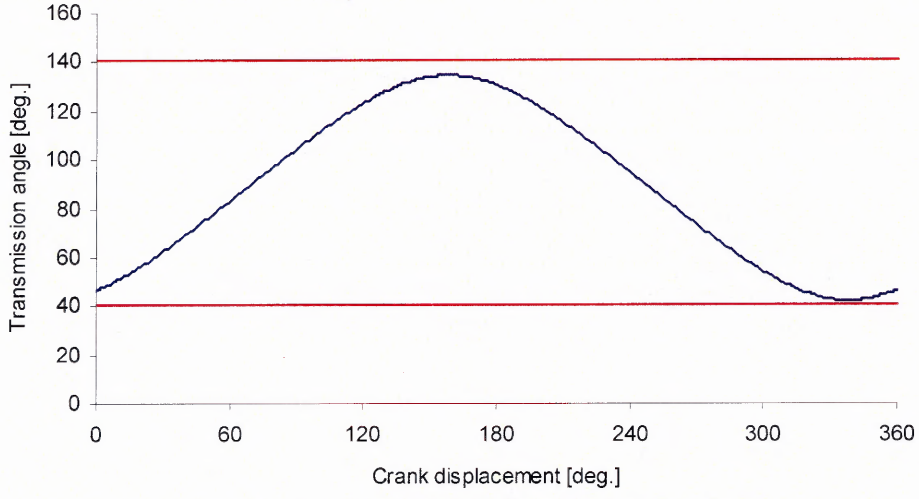

Figure 4.6 Transmission angles produced by optimized Grashof crank-rocker motion generator.

4.2 Optimized Grashof Drag Link Motion Generator

This example demonstrates the synthesis of a Grashof drag link motion generator with minimum perimeter and feasible transmission angles ($40° \leq \phi \leq 140°$) given a series of prescribed rigid-body positions.

Table 4.2 includes the prescribed point coordinates and displacement angles for four rigid-body positions. Given these rigid-body positions, fixed and moving pivot curves will be produced using the numerical method described in Section 2.3 (Block B1 in Figure 3.6 and Appendix B Section 1.1). Using the following range for variable m_x and initial guesses for m_y, k_x, k_y, R_1:

$$m_x = 0.5, 1.0, \ldots 5.0, m_y = -0.5, k_x = 0.5, k_y = 1.0, R_1 = 2.0$$

the fixed and moving pivot curves illustrated in Figure 4.7 are produced. As the prescribed increment for m_x decreases the number on data points for the fixed and moving pivot curves and subsequently, the number of available four-bar motion generator solutions increases.

Table 4.2 Prescribed Rigid-body Parameters

Rigid-Body Positions		
	P	***α°***
1	2.1949, 2.9022	
2	1.5406, 3.0443	4.8100
3	0.8728, 3.0498	10.1338
4	0.2208, 2.9234	16.0919
5	-0.3897, 2.6754	22.7946

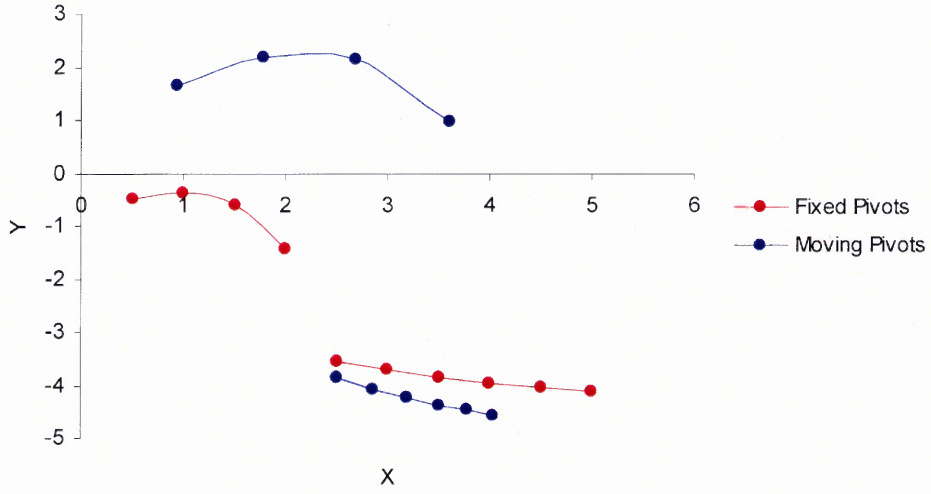

Figure 4.7 Fixed and moving pivot curves generated from data in Table 4.2.

From the output of Appendix B Section 1.2 (Block B2 in Figure 3.6), a plot of the crank/follower lengths of every four-bar motion generator solution in the fixed and moving pivot curves in Figure 4.7 is produced and illustrated in Figure 4.8. The abscissa in Figure 4.8 represents the sequentially assigned data point number and the ordinate represents the crank/follower length. The crank/follower length is the distance between each fixed pivot point and the corresponding moving pivot point.

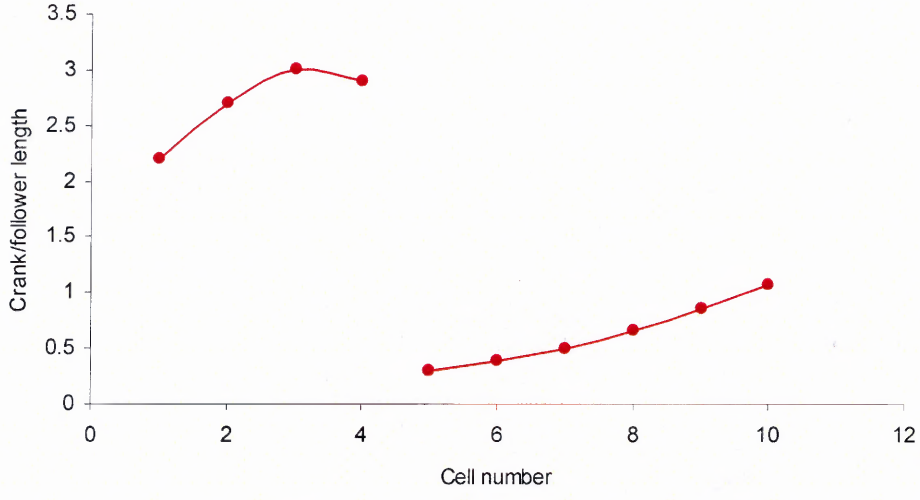

Figure 4.8 Crank/follower length solutions from fixed and moving pivot curves in Figure 4.7.

From the output of Appendix B Section 1.2 (Block B2 in Figure 3.6), surface plots of the coupler and ground lengths of every four-bar motion generator solution in the fixed and moving pivot curves in Figure 4.7 is produced and illustrated in Figure 4.9 and Figure 4.10, respectively. The horizontal and vertical axes in Figure 4.9 and Figure 4.10 are identical and represent the sequentially assigned data point number and the axis normal to the page represents the coupler length in Figure 4.9 and the ground length in Figure 4.10. The crank/follower length is the distance between each fixed pivot point and the corresponding moving pivot point. The coupler length is the distance between any two moving pivot points and the ground length is the distance between any two fixed pivot points.

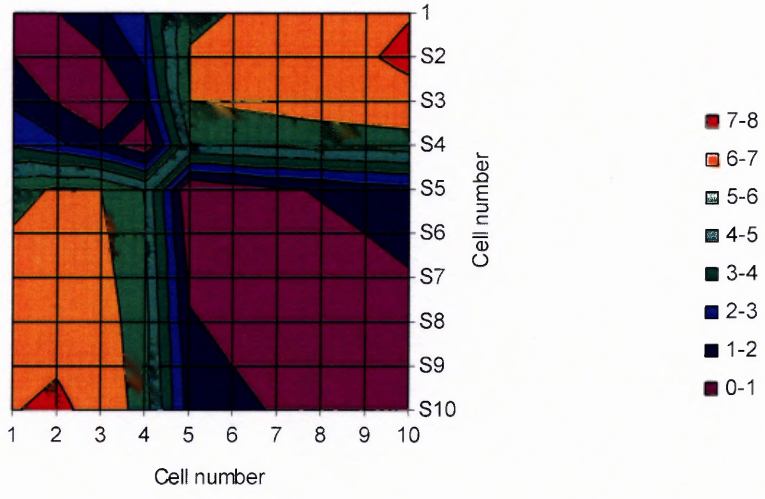

Figure 4.9 Coupler length solutions from fixed and moving pivot curves in Figure 4.7.

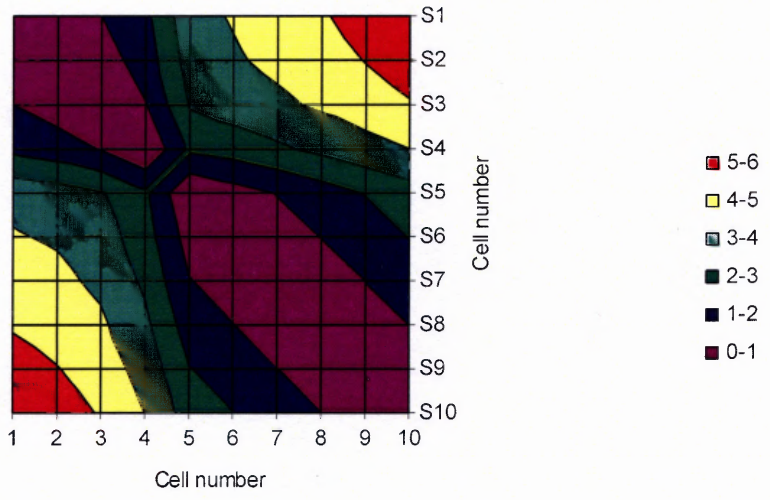

Figure 4.10 Ground length solutions from fixed and moving pivot curves in Figure 4.7.

Given such a potentially vast number of mechanism solutions, the numerical curve-based optimization algorithm presented in this work enables one to select an optimum motion generator solution with respect to Grashof criteria, mechanism perimeter and transmission angle criteria judiciously and efficiently.

After the transmission angle calculation stage and the down selection stages (Block B3 in Figure 3.6 and Appendix B Section 1.3), the fixed pivots, moving pivots and crank displacement angles for the optimized motion generator selected are produced in block B6 (Appendix B Section 1.6). The following are the fixed pivots, moving pivots and crank displacement angles for the optimized motion generator selected:

$\boldsymbol{m}$ = (2.000, -1.4431), $\boldsymbol{k}$ = (3.6147, 0.9465), $\boldsymbol{m}^*$ = (1.500, -0.6340), $\boldsymbol{k}^*$ = (2.6912, 2.1234)

The ground link (link $\boldsymbol{m}$-$\boldsymbol{m}^*$) has a length of 0.9511 units (therefore L_{min} = ground = 0.9511). The crank link (L_{max}) has a length of 3.0037 units. The sum of the remaining two links (the follower and coupler link) is 4.3801 units. According to Grashof criteria in Table 3.1, the optimized mechanism is indeed a drag link.

Figure 4.11 illustrates the optimized Grashof drag link motion generator. The graph in Figure 4.12 illustrates the transmission angles produced by the optimized Grashof drag link motion generator. Unlike the algebraic mechanism solutions associated with Burmester curves, mechanism solutions associated with numerically-generated fixed and moving pivot curves have a degree of structural error. Table 4.3 includes the rigid-body positions achieved by the optimized motion generator, the calculated structural error, the associated crank angle, and the coupler angle error. Figure 4.12 shows the transmission angle achieved by the synthesized motion generator in Figure 4.11 and are within the min/max transmission angle criteria ($40° \leq \phi \leq 140°$).

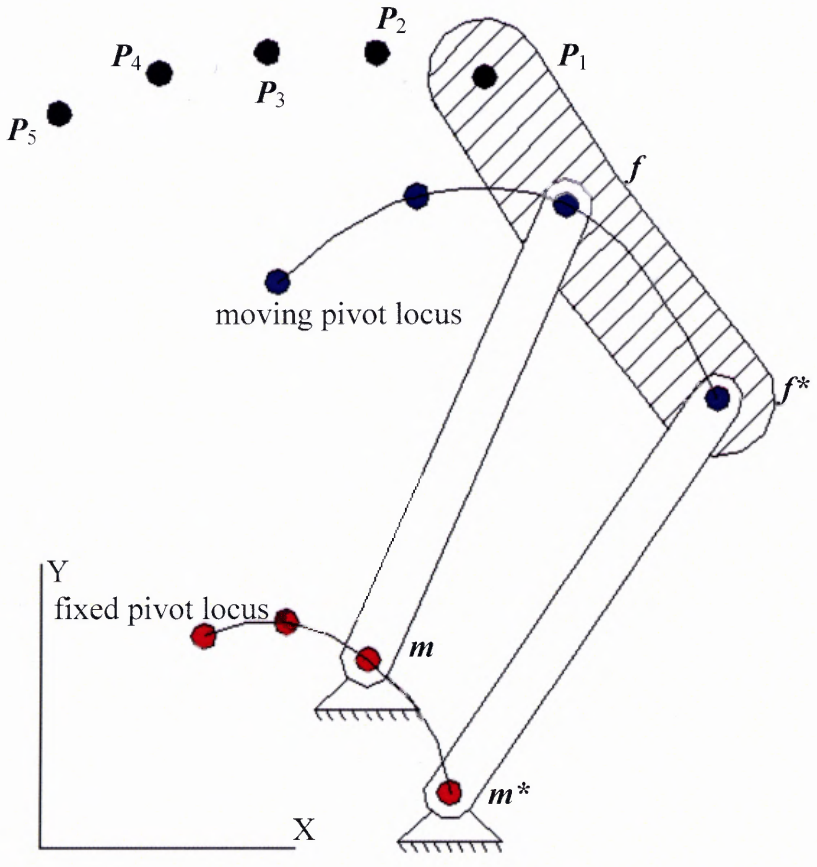

Figure 4.11 Optimized Grashof drag link motion generator.

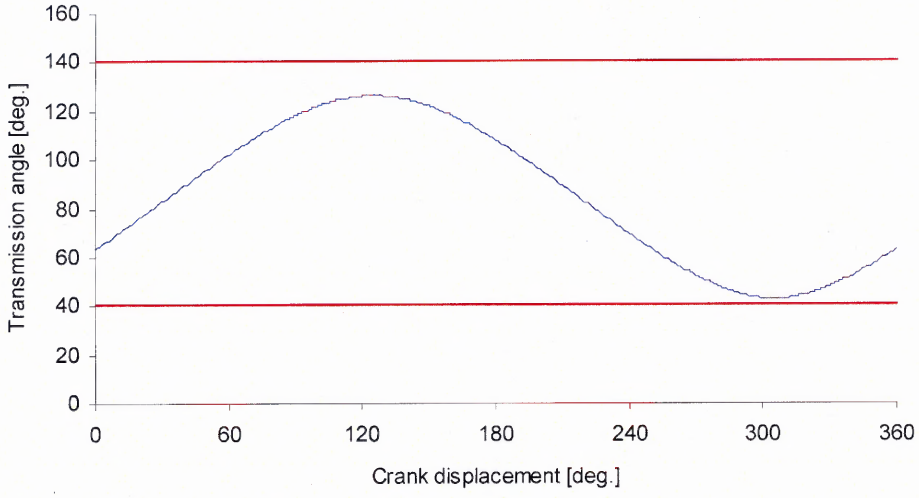

Figure 4.12 Transmission angles produced by optimized Grashof crank-rocker motion generator

Table 4.3 Rigid-body Positions Achieved by the Optimized Grashof Drag Link Motion Generator and Structural Error

Rigid-Body Position	*P*	Structural Error	Crank Angle $\theta°$	Coupler Angle Error
1	2.1949, 2.9022			
2	1.5518, 3.0418	0.0068	11.0000	0.0487
3	0.8871, 3.0499	0.0072	21.5000	0.0822
4	0.2208, 2.9221	0.0006	31.5000	0.0417
5	-0.3924, 2.6726	0.0027	40.5000	0.0783

4.3 Optimized Grashof Double Rocker Motion Generator

This example demonstrates the synthesis of a Grashof double rocker motion generator with minimum perimeter given a series of prescribed rigid-body positions.

Table 4.4 includes the prescribed point coordinates and displacement angles for four rigid-body positions. Given these rigid-body positions, fixed and moving pivot curves will be produced using the numerical method described in Section 2.3 (Block B1 in Figure 3.6 and Appendix B Section 1.1). Using the following range for variable m_x and initial guesses for m_y, k_x, k_y, R_1:

$m_x = 0.0, 0.2, \ldots 1.6, m_y = 0.1, k_x = 0.1, k_y = 1.0, R_1 = 1.0$

the fixed and moving pivot curves illustrated in Figure 4.13 are produced. As the prescribed increment for m_x decreases the number on data points for the fixed and moving pivot curves and subsequently, the number of available four-bar motion generator solutions increases.

Table 4.4 Prescribed Rigid-body Parameters

Rigid-Body Positions		
	P	α°
1	0.5728, 1.4741	
2	0.4085, 1.4473	-1.1491
3	0.2504, 1.3891	-2.4320
4	0.1046, 1.2989	-4.0113
5	-0.0217, 1.1749	-6.2624

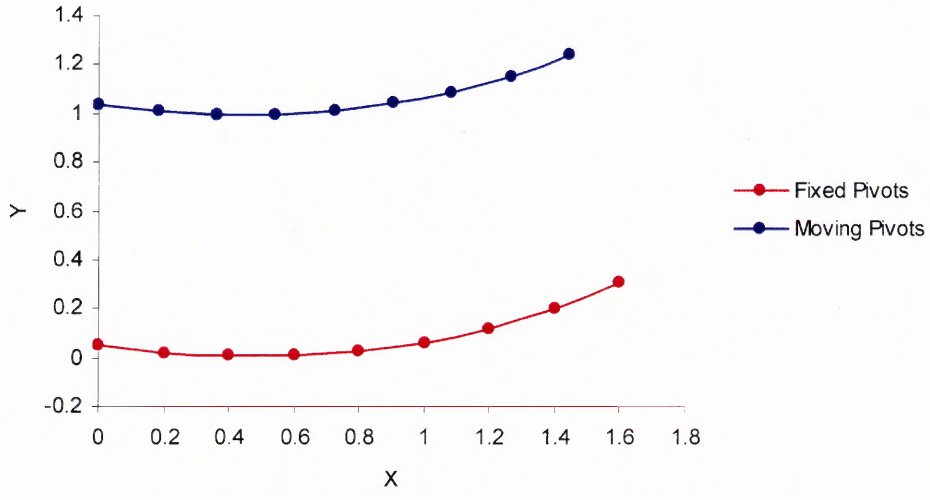

Figure 4.13 Fixed and moving pivot curves generated from data in Table 4.4.

From the output of Appendix B Section 1.2 (Block B2 in Figure 3.6), a plot of the crank/follower lengths of every four-bar motion generator solution in the fixed and moving pivot curves in Figure 4.13 is produced and illustrated in Figure 4.14. The abscissa in Figure 4.14 represents the sequentially assigned data point number and the

ordinate represents the crank/follower length. The crank/follower length is the distance between each fixed pivot point and the corresponding moving pivot point.

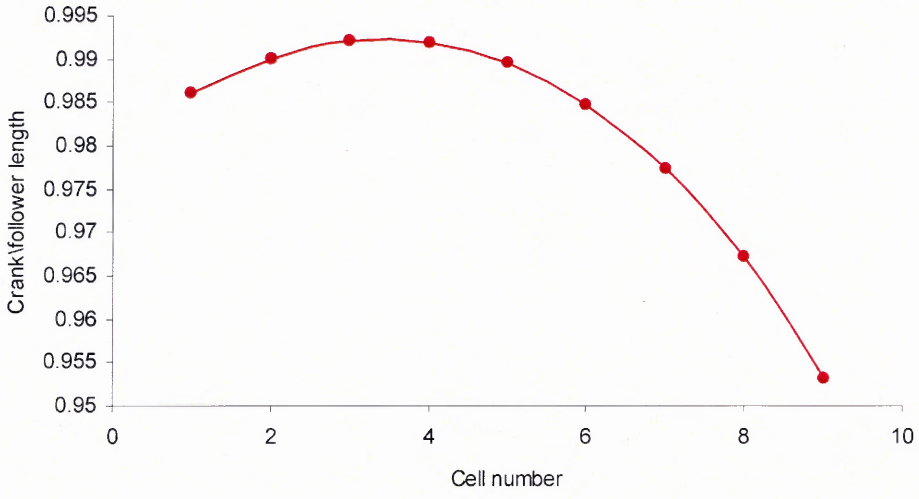

Figure 4.14 Crank/follower length solutions from fixed and moving pivot curves in Figure 4.13.

From the output of Appendix B Section 1.2 (block B2 in Figure 3.6), surface plots of the coupler and ground lengths of every four-bar motion generator solution in the fixed and moving pivot curves in Figure 4.13 is produced and illustrated in Figure 4.15 and Figure 4.16, respectively. The horizontal and vertical axes in Figure 4.15 and Figure 4.16 are identical and represent the sequentially assigned data point number and the axis normal to the page represents the coupler length in Figure 4.15 and the ground length in Figure 4.16. The crank/follower length is the distance between each fixed pivot point and the corresponding moving pivot point. The coupler length is the distance between any two moving pivot points and the ground length is the distance between any two fixed pivot points.

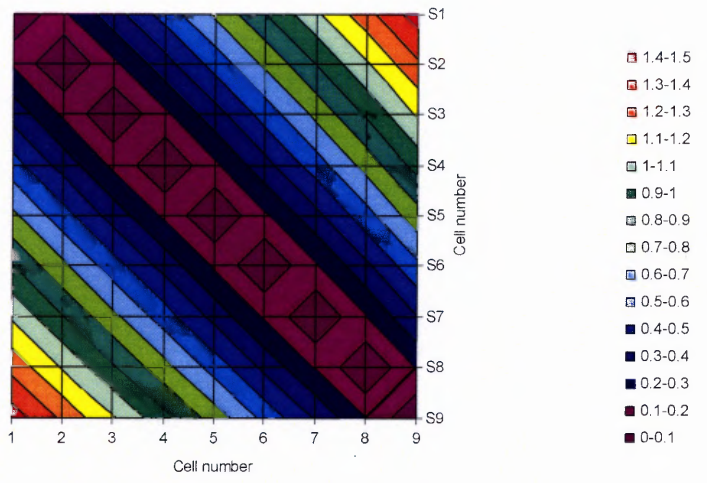

Figure 4.15 Coupler length solutions from fixed and moving pivot curves in Figure 4.13.

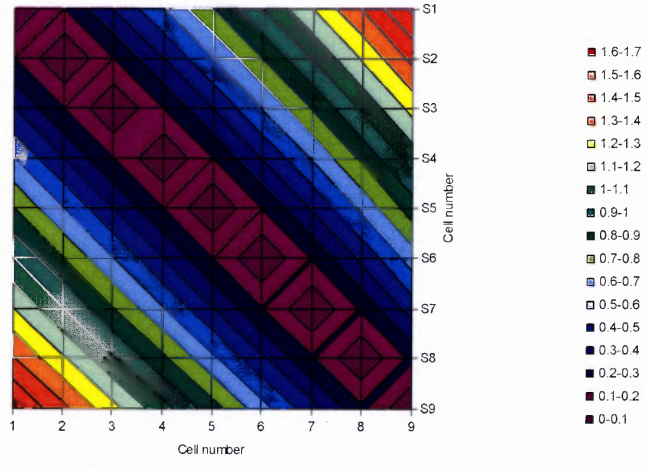

Figure 4.16 Ground length solutions from fixed and moving pivot curves in Figure 4.13.

Given such a potentially vast number of mechanism solutions, the numerical curve-based optimization algorithm presented in this work enables one to select an optimum motion generator solution with respect to Grashof criteria, mechanism perimeter and transmission angle criteria judiciously and efficiently.

After the transmission angle calculation stage and the down selection stages (Block B3 in Figure 3.6 and Appendix B Section 1.3), the fixed pivots, moving pivots and crank displacement angles for the optimized motion generator selected are produced in block

B6 (Appendix B Section 1.6). The following are the fixed pivots, moving pivots and crank displacement angles for the optimized motion generator selected:

$\boldsymbol{m}$ = (1.400, 0.1920), $\boldsymbol{k}$ = (1.2642, 1.1494), $\boldsymbol{m}^*$ = (1.600, 0.2968), $\boldsymbol{k}^*$ = (1.4457, 1.2373)

The coupler link (link $\boldsymbol{f}$-$\boldsymbol{f}^*$) has a length of 0.2017 units (therefore L_{min} = coupler = 0.2017). The crank link (L_{max}) has a length of 0.9669 units. The sum of the remaining two links (the follower and ground link) is 1.1789 units. According to Grashof criteria in Table 3.1, the optimized mechanism is indeed a double rocker.

Figure 4.17 illustrates the optimized Grashof double rocker motion generator. Unlike the algebraic mechanism solutions associated with Burmester curves, mechanism solutions associated with numerically-generated fixed and moving pivot curves have a degree of structural error. Table 4.5 includes the rigid-body positions achieved by the optimized motion generator, the associated crank angle and the calculated structural error.

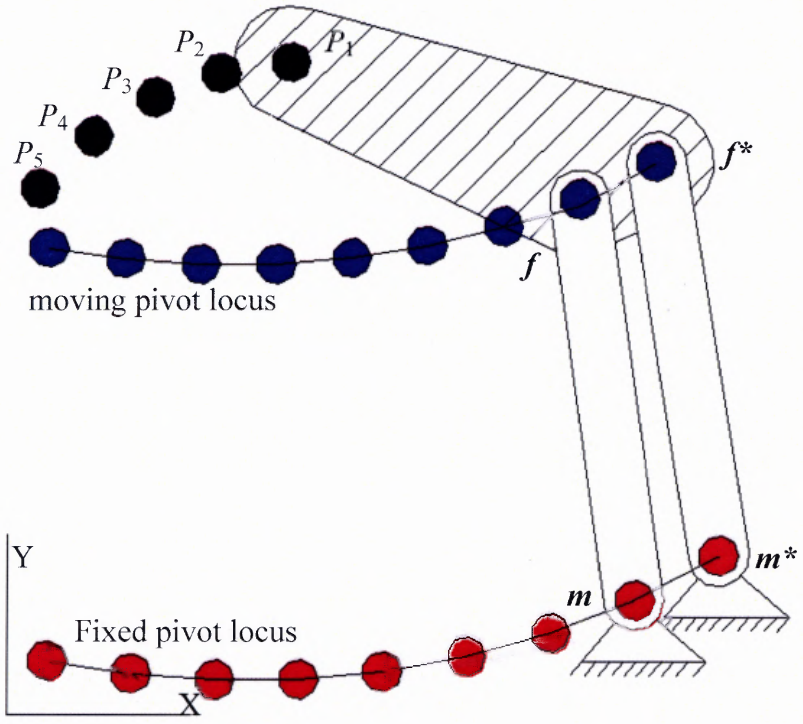

Figure 4.17 Optimized Grashof double rocker motion generator.

Table 4.5 Rigid-body Positions Achieved by the Optimized Grashof Double Rocker Motion Generator and Structural Error

Rigid-Body Position	P	Structural Error	Crank Angle $\theta°$	Coupler Angle Error
1	0.5728, 1.4741			
2	0.4088, 1.4475	0.0003	10.5000	0.0199
3	0.2496, 1.3889	0.0004	21.5000	0.0424
4	0.1041, 1.2988	0.0002	33.0000	0.0700
5	-0.0209, 1.1761	0.0010	45.5000	0.1088

4.4 Optimized Grashof Triple Rocker Motion Generator

This example demonstrates the synthesis of a Grashof triple rocker motion generator with minimum perimeter and feasible transmission angles ($40 \leq \phi$) given a series of prescribed rigid-body positions.

Table 4.6 includes the prescribed point coordinates and displacement angles for four rigid-body positions. Given these rigid-body positions, fixed and moving pivot curves will be produced using the Burmester method described in Section 2.2 (Block A1 in Figure 3.6 and Appendix A Section 1.1). Using the following range for variable β_2:

$$\beta_2 = 0.05, 0.1 \ldots 0.75 \text{ rad}$$

the fixed and moving pivot curves illustrated in Figure 4.18 are produced. As the prescribed increment for β_2 decreases the number on data points for the fixed and moving pivot curves and subsequently, the number of available four-bar motion generator solutions increases.

Table 4.6 Prescribed Rigid-body Parameters

Rigid-Body Positions			
	P	θ°	α°
1	1.4159, 1.9161	0	0
2	1.6345, 1.7778	3.6292	3.6292
3	1.6356, 1.6369	13.5386	13.5386
4	0.8147, 1.4919	51.8900	51.8900

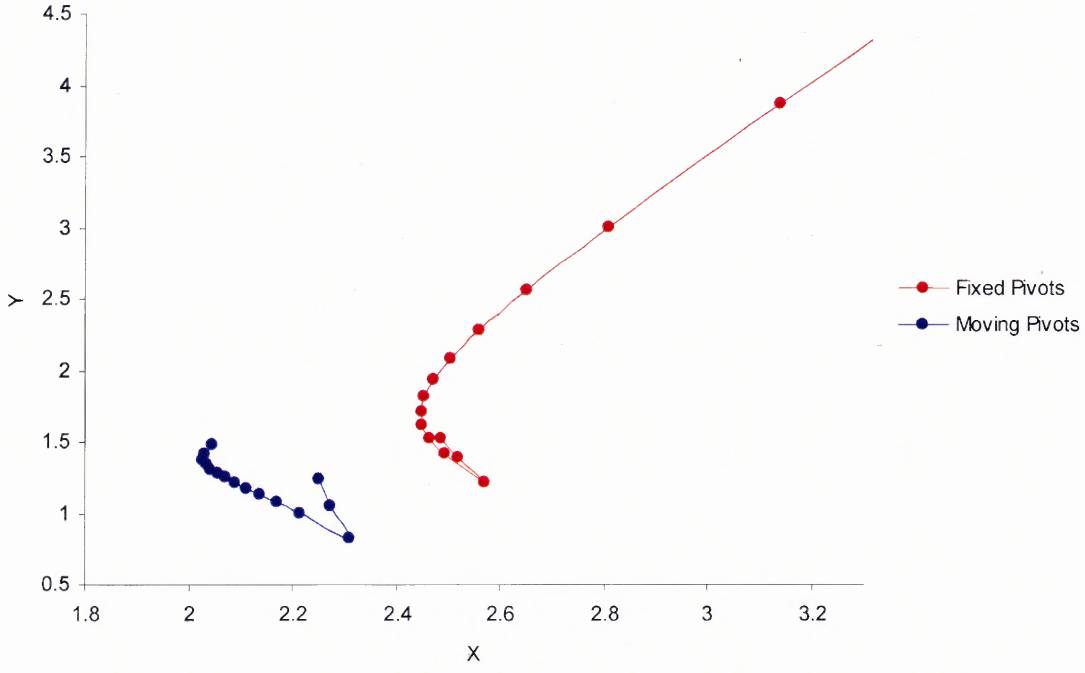

Figure 4.18 Fixed and moving pivot curves generated from data in Table 4.6.

From the output of Appendix A Section 1.2 (Block A2 in Figure 3.6), a plot of the crank/follower lengths of every four-bar motion generator solution in the fixed and moving pivot curves in Figure 4.18 is produced and illustrated in Figure 4.19. The abscissa in Figure 4.19 represents the sequentially assigned data point number and the ordinate represents the crank/follower length. The crank/follower length is the distance between each fixed pivot point and the corresponding moving pivot point.

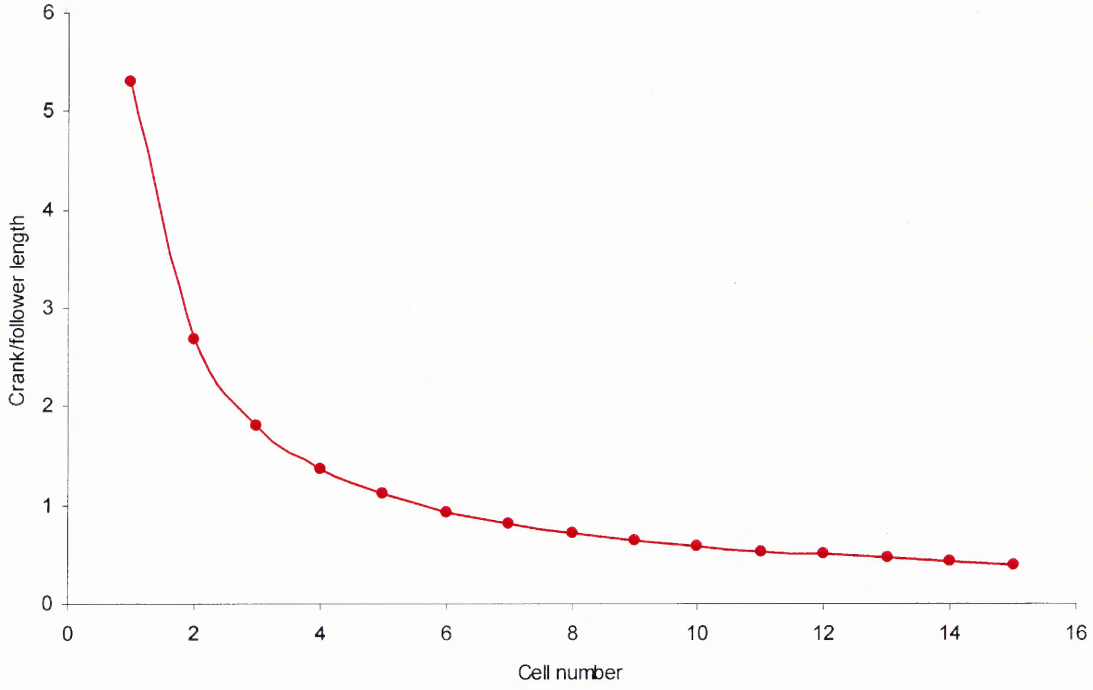

Figure 4.19 Crank/follower length solutions from fixed and moving pivot curves in Figure 4.18.

From the output of Appendix A Section 1.2 (Block A2 in Figure 3.6), surface plots of the coupler and ground lengths of every four-bar motion generator solution in the fixed and moving pivot curves in Figure 4.18 is produced and illustrated in Figure 4.20 and Figure 4.21, respectively. The horizontal and vertical axes in Figure 4.20 and Figure 4.21 are identical and represent the sequentially assigned data point number and the axis normal to the page represents the coupler length in Figure 4.20 and the ground length in Figure 4.21. The crank/follower length is the distance between each fixed pivot point and the corresponding moving pivot point. The coupler length is the distance between any two moving pivot points and the ground length is the distance between any two fixed pivot points.

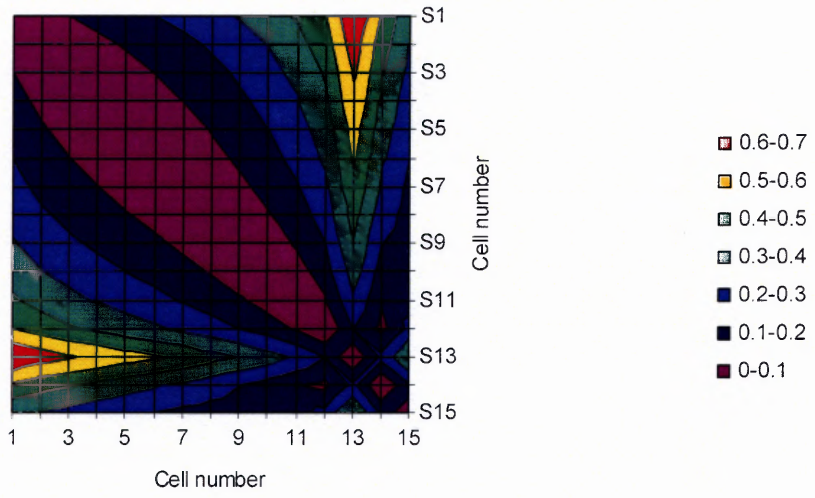

Figure 4.20 Coupler length solutions from fixed and moving pivot curves in Figure 4.18.

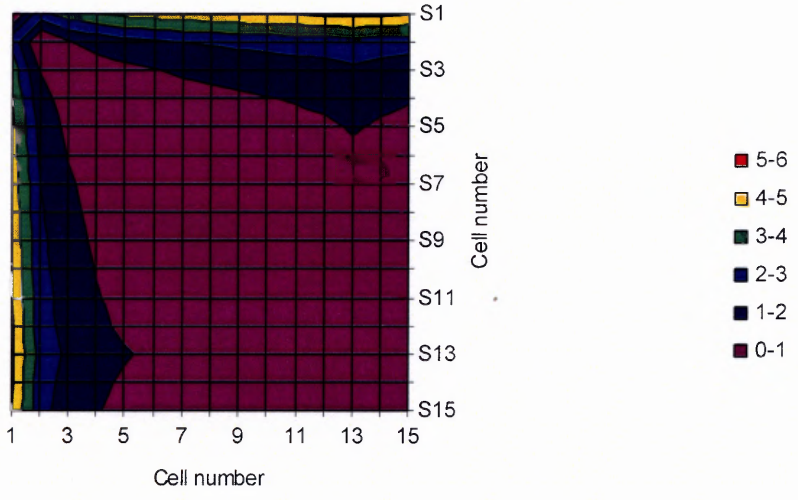

Figure 4.21 Ground length solutions from fixed and moving pivot curves in Figure 4.18.

Given such a potentially vast number of mechanism solutions, the Burmester curve-based optimization algorithm presented in this work enables one to select an optimum motion generator solution with respect to Grashof criteria, mechanism perimeter and transmission angle criteria judiciously and efficiently.

After the transmission angle calculation stage and the down selection stages (Block A3 in Figure 3.6 and Appendix A Section 1.3), the fixed pivots, moving pivots and crank displacement angles for the optimized motion generator selected are produced in block A6 (Appendix A Section 1.6). The following are the fixed pivots, moving pivots and crank displacement angles for the optimized motion generator selected:

$\boldsymbol{m}$ = (2.4636, 1.5093), $\boldsymbol{k}$ = (2.1710, 1.0746), $\boldsymbol{m}^*$ = (2.5205, 1.3781), $\boldsymbol{k}^*$ = (2.2717, 1.0469)

The displacement angles (rad) are required to achieve the prescribed rigid-body positions.

$$\beta_2 = 0.55000000, \beta_3 = 0.79053405, \beta_4 = 3.38192468$$

The coupler link (link $\boldsymbol{k}$-$\boldsymbol{k}^*$) has a length of 0.1044 units (therefore $L_{\min}$ = coupler = 0.1044). The crank link ($L_{\max}$) has a length of 0.5239 units. The sum of the remaining two links (the follower link and ground link) is 0.5572 units. According to Grashof criteria in Table 3.1, the optimized mechanism is indeed a triple rocker.

Figure 4.22 illustrates the optimized Grashof triple rocker motion generator. The graph in Figure 4.23 illustrates the transmission angles produced by the optimized Grashof triple rocker motion generator. Figure 4.22 shows the transmission angle achieved by the synthesized motion generator in Figure 4.22 and are within the min transmission angle criteria ($40° \leq \phi$) through the operation range of 158° to 317°.

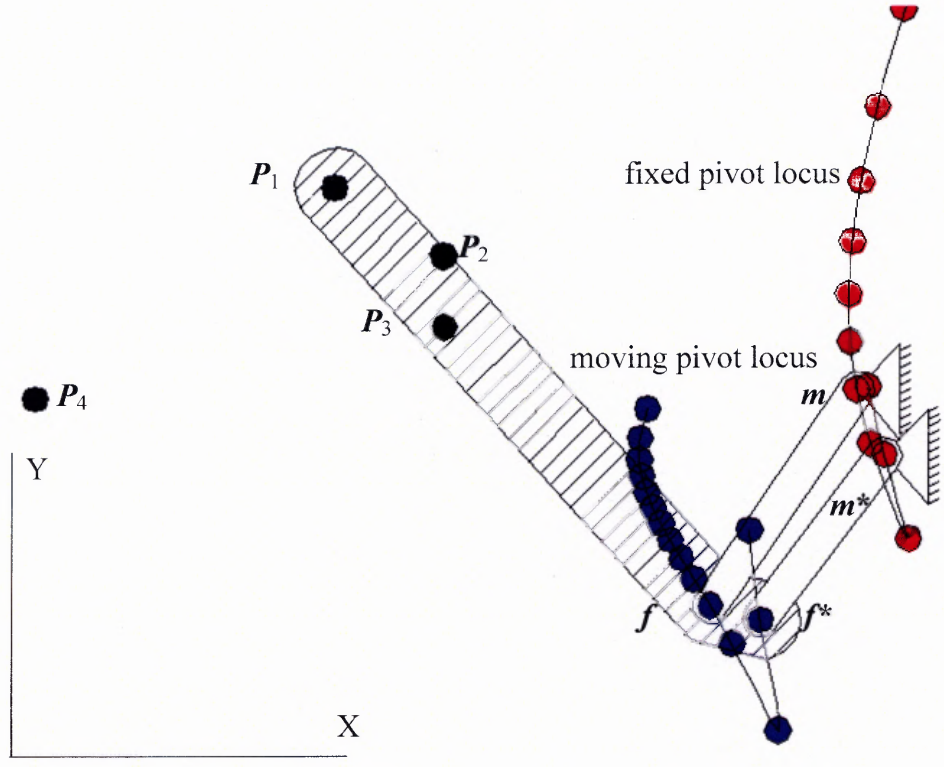

Figure 4.22 Optimized Grashof triple-rocker motion generator.

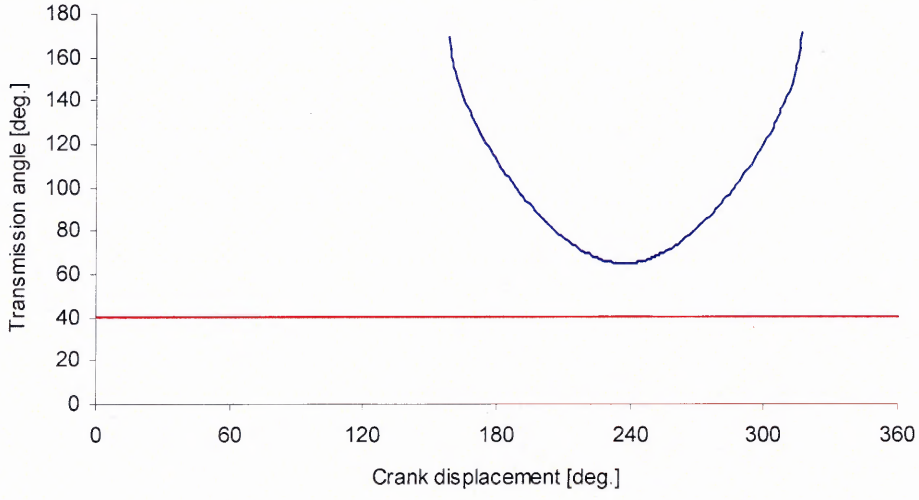

Figure 4.23 Transmission angles produced by optimized Grashof triple rocker motion generator.

CHAPTER 5

DISCUSSION

In this work, two distinct algorithms for selecting planar four-bar motion generators with respect to Grashof conditions, mechanism perimeter constraints and transmission angle constraints were developed and codified in MathCAD. In MathCAD, one can express numerical values to a precision of over ten decimal places. All of the data calculated in this work are specified to four decimal places. All calculated mechanism dimensions (linear dimensions only, not angular) are unit less and the word "unit" is often used as a suffix to describe them throughout the examples in this work.

Coordinate systems with X and Y labels for the abscissa and ordinate, respectively are used throughout this work. In the Burmester curve synthesis examples, the X-Y coordinate system is analogous to a Real-Imaginary coordinate system.

As written, the algorithms developed and codified in this work do not accommodate the Grashof change point mechanism (see Table 3.1). This mechanism is not discussed in the text either. A change point mechanism represents a theoretical mechanism solution. In real-world engineering design, the change point mechanism is not practical to design, implement or maintain. Although the algorithms do not accommodate the change point mechanism, the user can configure the codified algorithms to do so by incorporating change point mechanism conditions in Blocks A4 and B4.

All mechanism solutions via the numerical method contain a degree of structural error (unlike the Burmester method which produces analytical mechanism solutions). In this work, structural error is the average difference between the X and Y-components of the prescribed rigid-body points and those achieved by the synthesized mechanism. The coupler angle error is the difference between the prescribed rigid displacement angle and those achieved by the synthesized mechanism.

Although the algorithms developed and presented in this work were codified in MathCAD (because of availability and ease of use), the user is not necessarily limited to MathCAD. The user can codify the algorithms presented in this work in other platforms. Platforms such as C, C++, Mathematica, Matlab and Maple (among others) are well suited for the computationally intense operations required in the algorithms.

For the error check procedure in Section 6 of Appendix B, a four-bar displacement analysis model presented by Suh and Radcliffe [34] is used. In this model, the coupler angle displacement variable (labeled α by Suh and Radcliffe) is calculated using a quadratic equation (therefore two solutions of α are calculated). After performing the error check with both signs in the quadratic equation, the coupler angles that produce the smaller structural error values are used in the example problems.

It is highly likely that the Grashof double rocker will violate even the most liberal transmission angle criteria since the coupler link of the double rocker makes a complete rotation with respect to ground. The same can possibly hold true for the triple rocker (depending on which link is L_{min}). The codified algorithms in this work allow the user to activate or deactivate the transmission angle criteria and modify the minimum and maximum angles required.

CHAPTER 6

CONCLUSION

For a series of prescribed rigid-body positions, an infinite number of planar four-bar mechanism solutions exist. Sorting through the unlimited number of possible mechanism solutions to find one that ensures full link rotatibility, produces feasible transmission angles, and is as compact as possible can be a overwhelming given a set of Burmester curves or numerically-generated fixed and moving pivot curves. In this work, two algorithms are developed and presented by which the user can select optimum planar four-bar motion generators (optimum with respect to Grashof criteria, mechanism perimeter criteria and transmission angle criteria) from a set of all mechanism solutions produced by through either Burmester curves or numerically-generated fixed and moving curves. Both algorithms have been codified in MathCAD for enhanced analysis capabilities and ease of use. The examples in this work demonstrate the synthesis of compact planar, crank-rocker, drag link, double-rocker and triple-rocker four bar motion generators with feasible transmission angles.

APPENDIX A

BURMESTER CURVE MOTION GENERATION PROGRAM IN MATHCAD

A.1 Burmester Curve Motion Generation

This Appendix contains the MathCAD code used in this work. The algorithm incorporates fixed and moving pivot curves generated by Burmester synthesis. The algorithm in sections A.1.1 through A.1.6 searches fixed and moving pivot curves and produces the parameters of the optimum motion generator (optimum with respect to particular Grashof conditions, transmission angle constraints and mechanism perimeter constraints).

A.1.1 Generate and Input Burmester Fixed and Moving Pivot Curves

ENTER WHAT TYPE OF MECHANISM (1 for GRASHOF or 2 for NON-GRASHOF)
Mechanism :=

ENTER WHICH LINK IS TO BE THE SMALLEST (3 for CRANK, 4 for GROUND, 5 for COUPLER)
Link :=

FEASIBLE TRANSMISSION ANGLE CRITERIA (1 for YES or 2 for NO)
TANGLE :=

ENTER MIN AND MAX TRANSMISSION ANGLE (ADVISE 40<ϕ<140)
MIN := MAX :=

PRESCRIBED RIGID-BODY POSITIONS

Angle of Coupler	**Points on Coupler**
$angle_1$:=	$point_1$:=
$angle_2$:=	$point_2$:=
$angle_3$:=	$point_3$:=
$angle_4$:=	$point_4$:=

$$\alpha_2 := (angle_2 - angle_1)\cdot\frac{\pi}{180} \qquad \delta_2 := point_2 - point_1$$

$$\alpha_3 := (angle_3 - angle_1)\cdot\frac{\pi}{180} \qquad \delta_3 := point_3 - point_1$$

$$\alpha_4 := (angle_4 - angle_1)\cdot\frac{\pi}{180} \qquad \delta_4 := point_2 - point_1$$

START := STEP := END :=

bur :=

$$\Delta_2 \leftarrow \left|\begin{pmatrix} e^{i\cdot\alpha_3} - 1 & \delta_3 \\ e^{i\cdot\alpha_4} - 1 & \delta_4 \end{pmatrix}\right|$$

$$\Delta_3 \leftarrow -\left|\begin{pmatrix} e^{i\cdot\alpha_2} - 1 & \delta_2 \\ e^{i\cdot\alpha_4} - 1 & \delta_4 \end{pmatrix}\right|$$

$$\Delta_4 \leftarrow \left|\begin{pmatrix} e^{i\cdot\alpha_2} - 1 & \delta_2 \\ e^{i\cdot\alpha_3} - 1 & \delta_3 \end{pmatrix}\right|$$

$\Delta_1 \leftarrow -\Delta_2 - \Delta_3 - \Delta_4$

$var\_1 \leftarrow 0$

$var\_2 \leftarrow 0$

$var\_3 \leftarrow 0$

$var\_4 \leftarrow 0$

$var\_5 \leftarrow 0$

$var\_6 \leftarrow 0$

for $\beta_2 \in START, STEP..END$

$\Delta \leftarrow \Delta_1 + \Delta_2 \cdot e^{i\cdot\beta_2}$

$$M\Delta_1 \leftarrow \left|\begin{pmatrix} Re(\Delta_1) \\ Im(\Delta_1) \end{pmatrix}\right|$$

$$M\Delta_2 \leftarrow \left|\begin{pmatrix} Re(\Delta_2) \\ Im(\Delta_2) \end{pmatrix}\right|$$

$$M\Delta_3 \leftarrow \left|\begin{pmatrix} Re(\Delta_3) \\ Im(\Delta_3) \end{pmatrix}\right|$$

$$M\Delta_4 \leftarrow \left|\begin{pmatrix} Re(\Delta_4) \\ Im(\Delta_4) \end{pmatrix}\right|$$

$$M\Delta \leftarrow \left|\begin{pmatrix} Re(\Delta) \\ Im(\Delta) \end{pmatrix}\right|$$

$k_1 \leftarrow 0$

$k_2 \leftarrow -1$

$\theta_3 \leftarrow k_1 \cdot 2 \cdot \pi - k_2 \cdot a\cos\left(\frac{M\Delta_4^2 - M\Delta_3^2 - M\Delta^2}{2 \cdot M\Delta_3 \cdot M\Delta}\right)$

$\beta_3 \leftarrow \arg(\Delta) + \theta_3 - \arg(\Delta_3)$ if $Re(\theta_3) = Re(\theta_3) + Im(\theta_3)$

$\theta_4 \leftarrow a\cos\left(\frac{M\Delta_3^2 - M\Delta_4^2 - M\Delta^2}{2 \cdot M\Delta_4 \cdot M\Delta}\right)$

$\beta_4 \leftarrow \arg(\Delta) + \theta_4 - \arg(\Delta_4)$ if $Re(\theta_4) = Re(\theta_4) + Im(\theta_4)$

$M \leftarrow \begin{pmatrix} e^{i\cdot\beta_2(i)} - 1 & e^{i\cdot\alpha_2} - 1 \\ e^{i\cdot\beta_3(i)} - 1 & e^{i\cdot\alpha_3} - 1 \end{pmatrix}^{-1} \cdot \begin{pmatrix} \delta_2 \\ \delta_3 \end{pmatrix}$

$W \leftarrow M_0$

$Z \leftarrow M_1$

$R_1 \leftarrow point_1$

$k_1 \leftarrow R_1 - Z$

$m \leftarrow k_1 - W$

var_2 ← augment(var_2, k_1) if var_1 = 0

var_3 ← augment(var_3, m) if var_1 = 0

var_4 ← augment(var_4, β_2) if var_1 = 0

var_5 ← augment(var_5, β_3) if var_1 = 0

var_6 ← augment(var_6, β_4) if var_1 = 0

continue otherwise

stack(var_2, var_3, var_4, var_5, var_6)

k :=

k ← $bur_{0,1}$

for i ∈ 2..cols(bur) − 1

  k ← stack(k, $bur_{0,i}$)

k

m :=

m ← $bur_{1,1}$

for i ∈ 2..cols(bur) − 1

  m ← stack(m, $bur_{1,i}$)

m

Fixed and Moving Pivot Coordinates

mx := Re(m) my := Im(m) kx := Re(k) ky := Re(k)

A.1.2 Calculation of All Mechanism Solutions

Number of elements in array

i := 0..rows(m) − 1 j := 0..rows(m) − 1

LENGTH OF CRANK AND FOLLOWER

$$CRANK_i := \sqrt{(mx_i - kx_i)^2 + (my_i - ky_i)^2}$$

$$FOLLOWER_i := \sqrt{(mx_i - kx_i)^2 + (my_i - ky_i)^2}$$

LENGTH OF GROUND AND COUPLER

$$GROUND_{i,j} := \sqrt{(mx_i - mx_j)^2 + (my_i - my_j)^2}$$

$$COUPLER_{i,j} := \sqrt{(kx_i - kx_j)^2 + (ky_i - ky_j)^2}$$

A.1.3 Calculation of all Mechanisms with Feasible Transmission Angles

START := STEP := END :=

ANGLE :=

for $i \in 0..rows(COUPLER) - 1$

  for $j \in 0..rows(COUPLER) - 1$

$$u_i \leftarrow \begin{bmatrix} \dfrac{mx_i - kx_i}{\sqrt{(kx_i - mx_i)^2 + (ky_i - my_i)^2}} \\ \dfrac{my_i - ky_i}{\sqrt{(kx_i - mx_i)^2 + (ky_i - my_i)^2}} \end{bmatrix} \text{ if } i \neq j$$

$$v_j \leftarrow \begin{bmatrix} \dfrac{mx_j - mx_i}{\sqrt{(mx_j - mx_i)^2 + (my_j - my_i)^2}} \\ \dfrac{my_j - my_i}{\sqrt{(mx_j - mx_i)^2 + (my_j - my_i)^2}} \end{bmatrix} \text{ if } i \neq j$$

$$ANGLES_{i,j} \leftarrow a\cos\left(\frac{u_i \cdot v_j}{|u_i| \cdot |v_j|}\right) \text{ if } i \neq j$$

$$ANGLES_{i,j} \leftarrow 0 \text{ otherwise}$$

$var\_1 \leftarrow 0$

for $i \in 0..rows(COUPLER) - 1$

  for $j \in 0..rows(COUPLER) - 1$

    for $\delta \in START, STEP \cdot \left(\frac{\pi}{180}\right)..END \cdot \left(\frac{\pi}{180}\right)$

$$L \leftarrow (GROUND_{i,j})^2 + (CRANK_i)^2 - \left(2 \cdot GROUND_{i,j} \cdot CRANK_i \cdot \cos(ANGLES_{i,j} + \delta)\right)$$

trans $\leftarrow \operatorname{acos}\left[\dfrac{(\mathrm{COUPLER}_{i,j})^2+(\mathrm{FOLLOWER}_j)^2-(L)}{2\cdot \mathrm{COUPLER}_{i,j}\cdot \mathrm{FOLLOWER}_j}\right]$ if

$i \neq j \wedge \mathrm{COUPLER}_{i,j} \neq 0 \wedge \mathrm{FOLLOWER}_j \neq 0$

trans $\leftarrow 0$ otherwise

var_1 $\leftarrow$ augment(var_1, trans)

$\mathrm{ccolumns} \leftarrow 1+\left(\dfrac{\mathrm{END}}{\mathrm{STEP}}\right)$

$\mathrm{rrows} \leftarrow \mathrm{cols}(\mathrm{COUPLER})^2$

$M \leftarrow \mathrm{var\_1}_{0,1}$

for $i \in 2..\mathrm{ccolumns}$

$M \leftarrow \mathrm{stack}(M, \mathrm{var\_1}_{0,i})$

for $i \in 1..\mathrm{rrows}-1$

$Z \leftarrow \mathrm{var\_1}_{0,\mathrm{ccolumns}\cdot i+1}$

for $j \in 2..\mathrm{ccolumns}$

$Z \leftarrow \mathrm{stack}(Z, \mathrm{var\_1}_{0,\mathrm{ccolumns}\cdot i+j})$

$M \leftarrow \mathrm{augment}(M, Z)$

$M \leftarrow M^T$

for $i \in 0,1..\left(\dfrac{\mathrm{cols}(\mathrm{var\_1})-1}{\mathrm{ccolumns}}\right)-1$

for $j \in 0,1..\dfrac{\mathrm{END}}{\mathrm{STEP}}$

$P_{i,j} \leftarrow M_{i,j}$

if TANGLE = 1

if Mechanism = 2

$P_{i,j} \leftarrow M_{i,j}$ if

$\mathrm{Re}(M_{i,j}) > \left(\mathrm{MIN}\cdot\dfrac{\pi}{180}\right) \wedge \mathrm{Re}(M_{i,j}) < \left(\mathrm{MAX}\cdot\dfrac{\pi}{180}\right) \vee$

$\mathrm{Re}(M_{i,j}) = 0$

$P_{i,0} \leftarrow 0$ otherwise

if Mechanism = 1

$P_{i,0} \leftarrow 0$ if

$\mathrm{Re}(M_{i,j}) < \left(\mathrm{MIN}\cdot\dfrac{\pi}{180}\right) \vee \mathrm{Re}(M_{i,j}) > \left(\mathrm{MAX}\cdot\dfrac{\pi}{180}\right)$

$P_{i,j} \leftarrow M_{i,j}$ otherwise

$P_{i,j} \leftarrow M_{i,j}$ otherwise

array $\leftarrow (0 \quad 0 \quad 0 \quad 0)$

array_1 $\leftarrow (0 \quad 0 \quad 0 \quad 0)$

for $z \in 0..\text{rows}(P)-1$
  for $i \in 0..\text{rows}(\text{COUPLER})-1$
    for $j \in 0..\text{rows}(\text{COUPLER})-1$
      for $\delta \in 0$
        if $\text{COUPLER}_{i,j} \neq 0 \wedge \text{FOLLOWER}_j \neq 0$

$$\text{dummy} \leftarrow \text{acos}\left[\frac{\left[\left(\text{COUPLER}_{i,j}\right)^2+\left(\text{FOLLOWER}_j\right)^2-\left[\left(\text{GROUND}_{i,j}\right)^2+\left(\text{CRANK}_i\right)^2-\left(\begin{matrix}2\cdot\text{GROUND}_{i,j}\cdot\text{CRANK}_i\cdot\\ \cos\left(\text{ANGLES}_{i,j}+\delta\right)\end{matrix}\right)\right]}{2\cdot\text{COUPLER}_{i,j}\cdot\text{FOLLOWER}_j}\right]$$

$$\text{array} \leftarrow \text{augment}\left(\begin{matrix}\text{CRANK}_i,\text{COUPLER}_{i,j},\text{FOLLOWER}_j,\\ \text{GROUND}_{i,j}\end{matrix}\right)$$

if $\text{dummy}=P_{z,0}$

$\text{array\_1} \leftarrow \text{stack}(\text{array\_1},\text{array})$ if $\text{dummy}=P_{z,0}$

continue otherwise

array_1

$\text{CCRANK} := \text{ANGLE}^{\langle 0\rangle}$ $\quad$ $\text{CCOUPLER} := \text{ANGLE}^{\langle 1\rangle}$

$\text{FFOLLOWER} := \text{ANGLE}^{\langle 2\rangle}$ $\quad$ $\text{GGROUND} := \text{ANGLE}^{\langle 3\rangle}$

A.1.4 Down-select of Grashoff

Cell :=

$\text{array} \leftarrow (0 \quad 0 \quad 0 \quad 0)$

for $i \in 0..\text{rows}(\text{GGROUND})-1$

$$v \leftarrow \text{sort}\left(\begin{pmatrix}\text{CCRANK}_i\\ \text{CCOUPLER}_i\\ \text{FFOLLOWER}_i\\ \text{GGROUND}_i\end{pmatrix}\right)$$

$$\text{M1} \leftarrow \text{augment}\left(\begin{matrix}\text{CCRANK}_i,\text{CCOUPLER}_i,\text{FFOLLOWER}_i,\\ \text{GGROUND}_i\end{matrix}\right)$$

$\text{array} \leftarrow \text{stack}(\text{array},\text{M1})$ if $\text{CCRANK}_i = v_0 \wedge \text{Link}=3$

array ← stack(array, M1) if $GGROUND_i = v_0 \wedge Link = 4$
array ← stack(array, M1) if $CCOUPLER_i = v_0 \wedge Link = 5$
continue otherwise
array1 ← (0 0 0 0)
for $i \in 0..rows(array) - 1$
$v \leftarrow sort\left(\begin{pmatrix} array_{i,0} \\ array_{i,1} \\ array_{i,2} \\ array_{i,3} \end{pmatrix}\right)$
$M1 \leftarrow augment(array_{i,0}, array_{i,1}, array_{i,2}, array_{i,3})$
array1 ← stack(array1, M1) if $v_0 + v_3 < v_1 + v_2 \wedge Mechanism = 1$
array1 ← stack(array1, M1) if $v_0 + v_3 < v_1 + v_2 \wedge Mechanism = 2$
continue otherwise
array1

A.1.5 Down-select of Perimeter

SOLUTION WITH SMALLEST PERIMETER

Cell2 :=
perimeter ← ∞
M2 ← (0 0 0 0)
for $i \in 1..rows(Cell) - 1$
$Dummy\_Perimeter \leftarrow Cell_{i,0} + Cell_{i,1} + Cell_{i,2} + Cell_{i,3}$
$M1 \leftarrow augment(Cell_{i,0}, Cell_{i,1}, Cell_{i,2}, Cell_{i,3})$
M2 ← M1 if Dummy_Perimeter < perimeter
perimeter ← Dummy_Perimeter if Dummy_Perimeter < perimeter
continue otherwise
augment(M2, perimeter)

A.1.6 Optimized Motion Generator and Operating Parameters

FIXED AND MOVING PIVOTS FOR MECHANISM

Cell3 :=
for $i \in 0..rows(kx) - 1$
$Dummy\_Follower \leftarrow \sqrt{(mx_i - kx_i)^2 (my_i - my_i)^2}$
$array \leftarrow augment(mx_i, kx_i, my_i, ky_i)$

coordinates ← array if Dummy_Follower = $Cell2_{0,0}$
coordinates_1 ← array if Dummy_Follower = $Cell2_{0,2}$
continue otherwise
solution ← stack(coordinates, coordinates_1)

SOLUTION FOR ROTATION ANGLES

Cell4 :=
value ← 0
for i ∈ 0..rows(kx) − 1
value ← i if $mx_i = Cell3_{0,0}$
continue otherwise
value

β_2 β_3 β_4

$bur_{2,Cell4+1} =$ $bur_{3,Cell4+1} =$ $bur_{4,Cell4+1} =$

APPENDIX B

NUMERICAL MOTION GENERATION PROGRAM IN MATHCAD

B.1 Numerical Motion Generation

This Appendix contains the MathCAD code used in this work. The algorithm incorporates fixed and moving pivot curves generated by numerically-generated fixed and moving pivot curves. The algorithm in sections B.1.1 through B.1.6 searches fixed and moving pivot curves and produces the parameters of the optimum motion generator (optimum with respect to particular Grashof conditions, transmission angle constraints and mechanism perimeter constraints).

B.1.1 Generate and Input Numerical Fixed and Moving Pivot Curves

ENTER WHAT TYPE OF MECHANISM (1 for GRASHOF or 2 for NON-GRASHOF)
Mechanism :=

ENTER WHICH LINK IS TO BE THE SMALLEST (3 for CRANK, 4 for GROUND, 5 for COUPLER)
Link :=

FEASIBLE TRANSMISSION ANGLE CRITERIA (1 for YES or 2 for NO)
TANGLE :=

ENTER MIN AND MAX TRANSMISSION ANGLE (ADVISE $40<\phi<140$)
MIN := MAX :=

PRESCRIBED RIGID-BODY POSITIONS

$px_1 :=$ $px_2 :=$ $px_3 :=$ $px_4 :=$ $px_5 :=$

$py_1 :=$ $py_2 :=$ $py_3 :=$ $py_4 :=$ $py_5 :=$

$\alpha 12 :=$ $\alpha 13 :=$ $\alpha 14 :=$ $\alpha 15 :=$

DISPLACEMENT MATRICES

$$D12 := \begin{pmatrix} \cos(\alpha 12) & -\sin(\alpha 12) & px_2 - px_1 \cdot \cos(\alpha 12) + py_1 \cdot \sin(\alpha 12) \\ \sin(\alpha 12) & \cos(\alpha 12) & py_2 - px_1 \cdot \sin(\alpha 12) - py_1 \cdot \cos(\alpha 12) \\ 0 & 0 & 1 \end{pmatrix}$$

$$D13 := \begin{pmatrix} \cos(\alpha 13) & -\sin(\alpha 13) & px_3 - px_1 \cdot \cos(\alpha 13) + py_1 \cdot \sin(\alpha 13) \\ \sin(\alpha 13) & \cos(\alpha 13) & py_3 - px_1 \cdot \sin(\alpha 13) - py_1 \cdot \cos(\alpha 13) \\ 0 & 0 & 1 \end{pmatrix}$$

$$D14 := \begin{pmatrix} \cos(\alpha 14) & -\sin(\alpha 14) & px_4 - px_1 \cdot \cos(\alpha 14) + py_1 \cdot \sin(\alpha 14) \\ \sin(\alpha 14) & \cos(\alpha 14) & py_4 - px_1 \cdot \sin(\alpha 14) - py_1 \cdot \cos(\alpha 14) \\ 0 & 0 & 1 \end{pmatrix}$$

$$D15 := \begin{pmatrix} \cos(\alpha 15) & -\sin(\alpha 15) & px_5 - px_1 \cdot \cos(\alpha 15) + py_1 \cdot \sin(\alpha 15) \\ \sin(\alpha 15) & \cos(\alpha 15) & py_5 - px_1 \cdot \sin(\alpha 15) - py_1 \cdot \cos(\alpha 15) \\ 0 & 0 & 1 \end{pmatrix}$$

PRESCRIBED VALUES

end :=

i := 1..end

m0x(i) := i

INITIAL GUESSES

my := kx := ky := R1 :=

Given

$$\left[D12 \cdot \begin{pmatrix} kx \\ ky \\ 1 \end{pmatrix} - \begin{pmatrix} mx(i) \\ my \\ 1 \end{pmatrix}\right] \cdot \left[D12 \cdot \begin{pmatrix} kx \\ ky \\ 1 \end{pmatrix} - \begin{pmatrix} mx(i) \\ my \\ 1 \end{pmatrix}\right] - R1^2 = 0$$

$$\left[D13 \cdot \begin{pmatrix} kx \\ ky \\ 1 \end{pmatrix} - \begin{pmatrix} mx(i) \\ my \\ 1 \end{pmatrix}\right] \cdot \left[D13 \cdot \begin{pmatrix} kx \\ ky \\ 1 \end{pmatrix} - \begin{pmatrix} mx(i) \\ my \\ 1 \end{pmatrix}\right] - R1^2 = 0$$

$$\left[D14 \cdot \begin{pmatrix} kx \\ ky \\ 1 \end{pmatrix} - \begin{pmatrix} mx(i) \\ my \\ 1 \end{pmatrix}\right] \cdot \left[D14 \cdot \begin{pmatrix} kx \\ ky \\ 1 \end{pmatrix} - \begin{pmatrix} mx(i) \\ my \\ 1 \end{pmatrix}\right] - R1^2 = 0$$

$$\left[D15 \cdot \begin{pmatrix} kx \\ ky \\ 1 \end{pmatrix} - \begin{pmatrix} mx(i) \\ my \\ 1 \end{pmatrix}\right] \cdot \left[D15 \cdot \begin{pmatrix} kx \\ ky \\ 1 \end{pmatrix} - \begin{pmatrix} mx(i) \\ my \\ 1 \end{pmatrix}\right] - R1^2 = 0$$

F(i) := Find(my, kx, ky, R1)

CALCULATED SOLUTIONS FOR FIXED AND MOVING PIVOT COORDINATES

$mx_{i-1} := mx(i)$ $\quad my_{i-1} := F(i)_0$ $\quad kx_{i-1} := F(i)_1$ $\quad ky_{i-1} := F(i)_2$

B.1.2 Calculation of all Mechanism Solutions

Number of elements in array

$i := 0..end - 1$ $\quad j := 0..end - 1$

LENGTH OF CRANK AND FOLLOWER

$$CRANK_i := \sqrt{(mx_i - kx_i)^2 + (my_i - ky_i)^2}$$

$$FOLLOWER_i := \sqrt{(mx_i - kx_i)^2 + (my_i - ky_i)^2}$$

LENGTH OF GROUND AND COUPLER

$$GROUND_{i,j} := \sqrt{(mx_i - mx_j)^2 + (my_i - my_j)^2}$$

$$COUPLER_{i,j} := \sqrt{(kx_i - kx_j)^2 + (ky_i - ky_j)^2}$$

B.1.3 Calculation of all Mechanisms with Feasible Transmission Angles

START := $\quad$ STEP := $\quad$ END :=

ANGLE :=

for $i \in 0..rows(COUPLER) - 1$

for $j \in 0..rows(COUPLER) - 1$

$$u_i \leftarrow \begin{bmatrix} \dfrac{mx_i - kx_i}{\sqrt{(kx_i - mx_i)^2 + (ky_i - my_i)^2}} \\ \dfrac{my_i - ky_i}{\sqrt{(kx_i - mx_i)^2 + (ky_i - my_i)^2}} \end{bmatrix} \text{ if } i \neq j$$

$$v_j \leftarrow \begin{bmatrix} \dfrac{mx_j - mx_i}{\sqrt{(mx_j - mx_i)^2 + (my_j - my_i)^2}} \\ \dfrac{my_j - my_i}{\sqrt{(mx_j - mx_i)^2 + (my_j - my_i)^2}} \end{bmatrix} \text{ if } i \neq j$$

$$\text{ANGLES}_{i,j} \leftarrow \text{acos}\left(\frac{u_i \cdot v_j}{|u_i| \cdot |v_j|}\right) \text{ if } i \neq j$$

$$\text{ANGLES}_{i,j} \leftarrow 0 \text{ otherwise}$$

$$\text{var\_1} \leftarrow 0$$

for $i \in 0..\text{rows}(\text{COUPLER}) - 1$

  for $j \in 0..\text{rows}(\text{COUPLER}) - 1$

    for $\delta \in \text{START}, \text{STEP} \cdot \left(\frac{\pi}{180}\right)..\text{END} \cdot \left(\frac{\pi}{180}\right)$

$$L \leftarrow (\text{GROUND}_{i,j})^2 + (\text{CRANK}_i)^2 - \left(2 \cdot \text{GROUND}_{i,j} \cdot \text{CRANK}_i \cdot \cos(\text{ANGLES}_{i,j} + \delta)\right)$$

$$\text{trans} \leftarrow \text{acos}\left[\frac{(\text{COUPLER}_{i,j})^2 + (\text{FOLLOWER}_j)^2 - (L)}{2 \cdot \text{COUPLER}_{i,j} \cdot \text{FOLLOWER}_j}\right] \text{ if } i \neq j \wedge \text{COUPLER}_{i,j} \neq 0 \wedge \text{FOLLOWER}_j \neq 0$$

$$\text{trans} \leftarrow 0 \text{ otherwise}$$

$$\text{var\_1} \leftarrow \text{augment}(\text{var\_1}, \text{trans})$$

$$\text{ccolumns} \leftarrow 1 + \left(\frac{\text{END}}{\text{STEP}}\right)$$

$$\text{rrows} \leftarrow \text{cols}(\text{COUPLER})^2$$

$$M \leftarrow \text{var\_1}_{0,1}$$

for $i \in 2..\text{ccolumns}$

  $M \leftarrow \text{stack}(M, \text{var\_1}_{0,i})$

for $i \in 1..\text{rrows} - 1$

  $Z \leftarrow \text{var\_1}_{0,\text{ccolumns} \cdot i + 1}$

  for $j \in 2..\text{ccolumns}$

    $Z \leftarrow \text{stack}(Z, \text{var\_1}_{0,\text{ccolumns} \cdot i + j})$

  $M \leftarrow \text{augment}(M, Z)$

$$M \leftarrow M^T$$

for $i \in 0,1..\left(\frac{\text{cols}(\text{var\_1}) - 1}{\text{ccolumns}}\right) - 1$

  for $j \in 0,1..\frac{\text{END}}{\text{STEP}}$

    $P_{i,j} \leftarrow M_{i,j}$

    if TANGLE = 1

      if Mechanism = 2

        $P_{i,j} \leftarrow M_{i,j}$ if

$\mathrm{Re}(M_{i,j}) > \left(MIN \cdot \frac{\pi}{180}\right) \wedge \mathrm{Re}(M_{i,j}) < \left(MAX \cdot \frac{\pi}{180}\right) \vee$

$\mathrm{Re}(M_{i,j}) = 0$

$P_{i,0} \leftarrow 0$ otherwise

if Mechanism = 1

$P_{i,0} \leftarrow 0$ if

$\mathrm{Re}(M_{i,j}) < \left(MIN \cdot \frac{\pi}{180}\right) \vee \mathrm{Re}(M_{i,j}) > \left(MAX \cdot \frac{\pi}{180}\right)$

$P_{i,j} \leftarrow M_{i,j}$ otherwise

$P_{i,j} \leftarrow M_{i,j}$ otherwise

$array \leftarrow (0 \quad 0 \quad 0 \quad 0)$

$array\_1 \leftarrow (0 \quad 0 \quad 0 \quad 0)$

for $z \in 0..rows(P) - 1$

for $i \in 0..rows(COUPLER) - 1$

for $j \in 0..rows(COUPLER) - 1$

for $\delta \in 0$

if $COUPLER_{i,j} \neq 0 \wedge FOLLOWER_j \neq 0$

$$dummy \leftarrow a\cos\left[\frac{\left[(COUPLER_{i,j})^2 + (FOLLOWER_j)^2 - \left[(GROUND_{i,j})^2 + (CRANK_i)^2 - \left(2 \cdot GROUND_{i,j} \cdot CRANK_i \cdot \cos(ANGLES_{i,j} + \delta)\right)\right]\right]}{2 \cdot COUPLER_{i,j} \cdot FOLLOWER_j}\right]$$

$$array \leftarrow augment\left(\begin{matrix} CRANK_i, COUPLER_{i,j}, FOLLOWER_j, \\ GROUND_{i,j} \end{matrix}\right)$$

if $dummy = P_{z,0}$

$array\_1 \leftarrow stack(array\_1, array)$ if $dummy = P_{z,0}$

continue otherwise

$array\_1$

$CCRANK := ANGLE^{\langle 0 \rangle}$ $\quad$ $CCOUPLER := ANGLE^{\langle 1 \rangle}$

$FFOLLOWER := ANGLE^{\langle 2 \rangle}$ $\quad$ $GGROUND := ANGLE^{\langle 3 \rangle}$

B.1.4 Down-select of Grashoff

Cell :=

array ← (0 0 0 0)

for i ∈ 0..rows(GGROUND) − 1

  v ← sort((CCRANK_i ; CCOUPLER_i ; FFOLLOWER_i ; GGROUND_i))

  M1 ← augment(CCRANK_i , CCOUPLER_i , FFOLLOWER_i , GGROUND_i)

  array ← stack(array, M1) if CCRANK_i = v_0 ∧ Link = 3

  array ← stack(array, M1) if GGROUND_i = v_0 ∧ Link = 4

  array ← stack(array, M1) if CCOUPLER_i = v_0 ∧ Link = 5

  continue otherwise

array1 ← (0 0 0 0)

for i ∈ 0..rows(array) − 1

  v ← sort((array_{i,0} ; array_{i,1} ; array_{i,2} ; array_{i,3}))

  M1 ← augment(array_{i,0}, array_{i,1}, array_{i,2}, array_{i,3})

  array1 ← stack(array1, M1) if v_0 + v_3 < v_1 + v_2 ∧ Mechanism = 1

  array1 ← stack(array1, M1) if v_0 + v_3 < v_1 + v_2 ∧ Mechanism = 2

  continue otherwise

array1

B.1.5 Down-select of Perimeter

SOLUTION WITH SMALLEST PERIMETER

Cell2 :=

perimeter ← ∞

M2 ← (0 0 0 0)

for i ∈ 1..rows(Cell) − 1

  Dummy_Perimeter ← Cell_{i,0} + Cell_{i,1} + Cell_{i,2} + Cell_{i,3}

  M1 ← augment(Cell_{i,0}, Cell_{i,1}, Cell_{i,2}, Cell_{i,3})

  M2 ← M1 if Dummy_Perimeter < perimeter

perimeter ← Dummy_Perimeter if Dummy_Perimeter < perimeter
continue otherwise
augment(M2, perimeter)

B.1.6 Optimized Motion Generator and Operating Parameters

FIXED AND MOVING PIVOTS FOR MECHANISM

Cell3 :=
for $i \in 0..rows(kx)-1$
$Dummy\_Follower \leftarrow \sqrt{(mx_i - kx_i)^2 (my_i - my_i)^2}$
$array \leftarrow augment(mx_i, kx_i, my_i, ky_i)$
$coordinates \leftarrow array$ if $Dummy\_Follower = Cell2_{0,0}$
$coordinates\_1 \leftarrow array$ if $Dummy\_Follower = Cell2_{0,2}$
continue otherwise
if $Cell2_{0,0} < Cell2_{0,2}$
smallest ← coordinates
largest ← coordinates_1
otherwise
smallest ← coordinates_1
largest ← coordinates
stack(smallest, largest)

ERROR AND MOVING PIVOT COORDINATES

$mx := Cell3_{0,0}$ $\quad m1x := Cell3_{1,0}$ $\quad kx := Cell3_{0,1}$ $\quad k1x := Cell3_{1,1}$

$my := Cell_{0,2}$ $\quad m1y := Cell3_{1,2}$ $\quad ky := Cell3_{0,3}$ $\quad k1y := Cell3_{1,3}$

$$m := \begin{pmatrix} mx \\ my \\ 1 \end{pmatrix} \quad m1 := \begin{pmatrix} m1x \\ m1y \\ 1 \end{pmatrix} \quad k := \begin{pmatrix} kx \\ ky \\ 1 \end{pmatrix} \quad k1 := \begin{pmatrix} k1x \\ k1y \\ 1 \end{pmatrix}$$

COUPLER POINTS

$p1x := px_1$

$p1y := py_1$

$$p1 := \begin{pmatrix} p1x \\ p1y \\ 1 \end{pmatrix}$$

ERROR

CCell :=

$error_2 \leftarrow \infty$

$error_3 \leftarrow \infty$

$error_4 \leftarrow \infty$

$error_5 \leftarrow \infty$

for $i \in 2..5$

for $j \in 0,0.5 \cdot \left(\frac{\pi}{180}\right)..360 \cdot \left(\frac{\pi}{180}\right)$

$$R \leftarrow \begin{pmatrix} \cos(\theta) & -\sin(\theta) & 0 \\ \sin(\theta) & \cos(\theta) & 0 \\ 0 & 0 & 1 \end{pmatrix}$$

$a \leftarrow R \cdot (k - m) + m$

$plp \leftarrow R \cdot (pl - m) + m$

$klp \leftarrow R \cdot (kl - m) + m$

$$P \leftarrow \begin{pmatrix} 0 & -1 & 0 \\ 1 & 0 & 0 \\ 0 & 0 & 1 \end{pmatrix}$$

$$Q \leftarrow \begin{pmatrix} 0 & 0 & 0 \\ 0 & 0 & 0 \\ 0 & 0 & 1 \end{pmatrix}$$

$$I \leftarrow \begin{pmatrix} 1 & 0 & 0 \\ 0 & 1 & 0 \\ 0 & 0 & 1 \end{pmatrix}$$

$E \leftarrow (a - ml) \cdot [(I - Q) \cdot (klp - a)]$

$F \leftarrow (a - ml) \cdot [P \cdot (klp - a)]$

$$G \leftarrow (a - ml) \cdot [Q \cdot (klp - a)] + \frac{1}{2}\left[\begin{matrix}(klp - a) \cdot (klp - a) + (a - ml) \cdot \\ (a - ml) - (kl - ml) \cdot (kl - ml)\end{matrix}\right]$$

$$\alpha \leftarrow 2 \cdot \operatorname{atan}\left[\frac{-F \pm \sqrt{(E^2 + F^2 - G^2)}}{G - E}\right]$$ **Refer to Chapter 5 for explanation**

$$R\alpha \leftarrow \begin{pmatrix} \cos(\alpha) & -\sin(\alpha) & 0 \\ \sin(\alpha) & \cos(\alpha) & 0 \\ 0 & 0 & 1 \end{pmatrix}$$

$b \leftarrow R\alpha \cdot (klp - a) + a$

$p \leftarrow R\alpha \cdot (plp - a) + a$

$p2x \leftarrow px_i$

$p2y \leftarrow py_i$

$$p2 \leftarrow \begin{pmatrix} p2x \\ p2y \\ 1 \end{pmatrix}$$

$$Dummy\_error \leftarrow \frac{|p_0 - p2_0| + |p_1 - p2_1|}{2}$$

$$u \leftarrow \begin{bmatrix} \frac{p_0 - a_0}{\sqrt{(p_0 - a_0)^2 + (p_1 - a_1)^2}} \\ \frac{p_1 - a_1}{\sqrt{(p_0 - a_0)^2 + (p_1 - a_1)^2}} \end{bmatrix}$$

$$v \leftarrow \begin{bmatrix} \frac{pl_0 - k_0}{\sqrt{(pl_0 - k_0)^2 + (pl_1 - k_1)^2}} \\ \frac{pl_1 - k_1}{\sqrt{(pl_0 - k_0)^2 + (pl_1 - k_1)^2}} \end{bmatrix}$$

$$ANG\_VAR \leftarrow a\cos\left(\frac{u \cdot v}{|u| \cdot |v|}\right)$$

$ANG_i \leftarrow ANG\_VAR$ if $Dummy\_error < error_i \wedge Re(\alpha) = Re(\alpha) + Im(\alpha)$

$new\_p_i \leftarrow p_0$ if $Dummy\_error < error_i \wedge Re(\alpha) = Re(\alpha) + Im(\alpha)$

$new\_p_i \leftarrow p_1$ if $Dummy\_error < error_i \wedge Re(\alpha) = Re(\alpha) + Im(\alpha)$

$angle_i \leftarrow \theta$ if $Dummy\_error < error_i \wedge Re(\alpha) = Re(\alpha) + Im(\alpha)$

$error_i \leftarrow Dummy\_error$ if $Dummy\_error < error_i \wedge Re(\alpha) = Re(\alpha) + Im(\alpha)$

continue otherwise

$$\left|\begin{array}{l}\text{stack}\left[\begin{array}{l}\text{augment}\left[\begin{array}{l}\text{new\_p}_2,\text{neww\_p}_2,\text{error}_2,\left(\text{angle}_2\cdot\frac{180}{\pi}\right),\\ \left(\left|\text{ANG}_2-\alpha 12\right|\cdot\frac{180}{\pi}\right)\end{array}\right],\\ \text{augment}\left[\begin{array}{l}\text{new\_p}_3,\text{neww\_p}_3,\text{error}_3,\left(\text{angle}_3\cdot\frac{180}{\pi}\right),\\ \left(\left|\text{ANG}_3-\alpha 13\right|\cdot\frac{180}{\pi}\right)\end{array}\right],\\ \text{augment}\left[\begin{array}{l}\text{new\_p}_4,\text{neww\_p}_4,\text{error}_4,\left(\text{angle}_4\cdot\frac{180}{\pi}\right),\\ \left(\left|\text{ANG}_4-\alpha 14\right|\cdot\frac{180}{\pi}\right)\end{array}\right],\\ \text{augment}\left[\begin{array}{l}\text{new\_p}_5,\text{neww\_p}_5,\text{error}_5,\left(\text{angle}_5\cdot\frac{180}{\pi}\right),\\ \left(\left|\text{ANG}_5-\alpha 15\right|\cdot\frac{180}{\pi}\right)\end{array}\right]\end{array}\right]\end{array}\right|$$

CCELL =

REFERENCES

1. Zhixing, W., Hongying, Y., Dewei, T., and Jiansheng, L., 2002, "Study on Rigid-body Guidance Synthesis of Planar Linkage," Mechanism and Machine Theory, **37**(7), pp. 673-684.

2. Akhras, R., and Angeles, J., 1990, "Unconstrained Nonlinear Least-square Optimization of Planar Linkages for Rigid-body Guidance," Mechanism and Machine Theory, **25**(1), pp. 97-118.

3. Vasiliu, A., and Yannou, B., 2001, "Dimensional Synthesis of Planar Mechanisms using Neural Networks: Application to Path Generator Linkages," Mechanism and Machine Theory, **36**(2), pp. 299-310.

4. Marín, F., and González, A., 2003, "Global Optimization in Path Synthesis Based on Design Space Reduction," Mechanism and Machine Theory, **38**(6), pp. 579-594.

5. Sancibrian, R., Viadero, F., García, P., and Fernández, A., 2004, "Gradient-based Optimization of Path Synthesis Problems in Planar Mechanisms," Mechanism and Machine Theory, **39**(8), pp. 839-856.

6. Tong, S., and Chiang, C. H., 1992, "Syntheses of Planar and Spherical Four-bar Path Generators by the Pole Method," Mechanism and Machine Theory, **27**(2), pp. 143-155.

7. Nolle, H., and Hunt, K. H., 1971, "Optimum Synthesis of Planar Linkages to Generate Coupler Curves," Journal of Mechanisms, **6**(3), pp. 267-287.

8. Shi, Z., Yang, X., Yang, W., and Cheng, Q., 2005, "Robust Synthesis of Path Generating Linkages," Mechanism and Machine Theory, **40**(1), pp. 45-54.

9. Chiang, C. H., 1975, "Synthesis of Four-bar Function Generators by means of Equations of Three Relative Poles—1. Finitely Separated Positions," Mechanism and Machine Theory, **10**(1), pp. 81-91.

10. Rao, A. C., 1979, "Synthesis of 4-bar Function-generators using Geometric Programming," Mechanism and Machine Theory, **14**(2), pp. 141-149.

11. Alizade, R. I., Novruzbekov, I. G., and Sandor, G. N., 1975, "Optimization of Four-bar Function Generating Mechanisms using Penalty Functions with Inequality and Equality Constraints," Mechanism and Machine Theory, **10**(4), pp. 327-336.

12. Bagci, C., 1976, "Optimum Synthesis of Planar Function Generators by the Linear Partition of the Dyadic Loop Equations," Mechanism and Machine Theory, **11**(1), pp. 33-46.

13. Sandgren, E., 1990, "A Multi-objective Design Tree Approach for the Optimization of Mechanisms," Mechanism and Machine Theory, **25**(3), pp. 257-272.

14. Simionescu, P. A., and Beale, D., 2002, "Optimum Synthesis of the Four-bar Function Generator in its Symmetric Embodiment: the Ackermann Steering Linkage," Mechanism and Machine Theory, **37**(12), pp. 1487-1504.

15. Bagci, C., and Rieser, G. M., 1984, "Optimum Synthesis of Function Generators Involving Derivative Constraints," Mechanism and Machine Theory, **19**(1), pp. 157-164.

16. Cabrera, J. A., Simon, A., and Prado, M., 2002, "Optimal Synthesis of Mechanisms with Genetic Algorithms," Mechanism and Machine Theory, **37**(10), pp. 1165-1177.

17. Cossalter, V., Doria, A., and Pasini, M., 1992, "A Simple Numerical Approach for Optimum Synthesis of a Class of Planar Mechanisms," Mechanism and Machine Theory, **27**(3), pp. 357-366.

18. Krishnamurty, S., and Turcic, D. A., 1992, "Optimal Synthesis of Mechanisms using Nonlinear Goal Programming Techniques," Mechanism and Machine Theory, **27**(5), pp. 599-612.

19. Sutherland, G. H., and Siddall, J. N., 1974, "Dimensional Synthesis of Linkages by Multifactor Optimization," Mechanism and Machine Theory, **9**(1), pp. 81-95.

20. Avilés, J., Hernández, A., and Amezua, E., 1995, "Nonlinear Optimization of Planar Linkages for Kinematic Syntheses," Mechanism and Machine Theory, **30**(4), pp. 501-518.

21. Erdman, A. G., 1981, "Three and Four Precision Point Kinematic Synthesis of Planar Linkages," Mechanism and Machine Theory, **16**(3), pp. 227-245.

22. Da Lio, M., Cossalter, V., and Lot, R., 2000, "On the use of Natural Coordinates in Optimal Synthesis of Mechanisms," Mechanism and Machine Theory, **35**(10), pp. 1367-1389.

23. Sancibrian, R., García, P., Viadero, F., and Fernández, A., (In Press), "A General Procedure Based on Exact Gradient Determination in Dimensional Synthesis of Planar Mechanisms," Mechanism and Machine Theory.

24. Fernández-Bustos, I., Aguirrebeitia, J., Avilés, R., and Angulo, C., (In Press), "Kinematical Synthesis of 1-dof Mechanisms using Finite Elements and Genetic Algorithms," Finite Elements in Analysis and Design.

25. Alba, J. A., Doblaré, M., and Gracia, L., 2000, "A Simple Method for the Synthesis of 2D and 3D Mechanisms with Kinematic Constraints," Mechanism and Machine Theory, **35**(5), pp. 645-674.

26. Khare, A. K., and Dave, R. K., 1979, "Optimizing 4-bar Crank-rocker Mechanism," Mechanism and Machine Theory, **14**(5), pp. 319-325.

27. Lebedev, P. A., 2003, "Vector Method for the Synthesis of Mechanisms," Mechanism and Machine Theory, **38**(3), pp. 265-276.

28. Khare, A. K., and Dave, R. K., 1980, "Synthesis of Double-rocker Mechanism with Optimum Transmission Characteristics," Mechanism and Machine Theory, **15**(2), pp. 77-80.

29. Sun, J. W. H., and Waldron, K. J., 1981, "Graphical Transmission Angle Control in Planar Linkage Synthesis," Mechanism and Machine Theory, **16**(4), pp. 385-397.

30. Waldron, K. J., 1978, "Location of Burmester Synthesis Solutions with Fully Rotatable Cranks," Mechanism and Machine Theory, **13**(2), pp. 125-137.

31. Chen, F. Y., 1969, "Position Synthesis of the Double-rocker Mechanism," Journal of Mechanisms, **4**(4), pp. 303-310.

32. Sandor, George N., and Erdman, Arthur G., 1984, *Advanced Mechanism Design: Analysis and Synthesis*, Prentice-Hall, INC., New Jersey.

33. Wilson, Charles E., and Sadler, J. Peter, 1993, *Kinematics and Dynamics of Machinery, 2nd Edition*, HarperCollins College Publishers, New York.

34. Suh, C.H., and Radcliffe, C.W., 1978, *Kinematics and Mechanism Design*, John Wiley and Sons, New York.